DOI: 10.1002/ejic.200900358

Metal Complexes of 4,11-Dimethyl-1,4,8,11-tetraazacyclotetradecane-1,8-bis(methylphosphonic acid) – Thermodynamic and Formation/Decomplexation Kinetic Studies

Ivona Svobodová,[a,b] Jana Havlíčková,[c] Jan Plutnar,[c] Přemysl Lubal,*[a] Jan Kotek,*[c] and Petr Hermann[c]

Keywords: Cyclam derivatives / Copper / Kinetics / Macrocyclic ligands / Stability constants

The macrocyclic ligand with two methylphosphonic acid pendant arms, 4,11-dimethyl-1,4,8,11-tetraazacyclotetradecane-1,8-bis(methylphosphonic acid) (1,8-H_4^{Me2}te2p, $H_4\mathbf{L^3}$), was synthesized by a new simple approach. The product of the reaction of quarternized formaldehyde cyclam aminal with the sodium salt of diethyl phosphite was hydrolyzed to give a very high yield of the title ligand. The $(H_6\mathbf{L^3})^{2+}$ cation in the solid state is protonated on all ring nitrogen atoms and on each phosphonate group. In the solid-state structure of $[Cu(H_3\mathbf{L^3})][Cu(H_2\mathbf{L^3})]PF_6{\cdot}3H_2O$, neutral as well as positively charged complex species are present. Molecular structures of both species are very similar having the copper(II) ion in a coordination environment between square-pyramidal and trigonal-bipyramidal arrangements (τ = 0.43 and 0.48) with one pendant arm non-coordinated. The ligand forms stable complexes with transition-metal ions showing a high selectivity for divalent copper atoms. The formation of complexes of the ligand with Cu^{II}, Zn^{II} and Cd^{II} is fast, confirming the acceleration of complexation due to the presence of the strongly coordinating pendant arms. Acid-assisted decomplexation is fast for all three metal ions. Therefore, the copper(II) complex is not suitable for medicinal applications employing copper radioisotopes, but the title ligand motive can be employed in copper(II) separation.

Introduction

Investigations of thermodynamically highly stable and kinetically inert complexes (often formed by macrocyclic ligands)[1–3] have been stimulated by their applications in several areas, for example as the contrast agents (CA) in magnetic resonance imaging (MRI)[4–8] or for labelling of biomolecules with metal radioisotopes for both diagnostic and therapeutic purposes.[9–13] In the above-mentioned medicinal utilizations, the harmful metal ion or radioisotope may not be deposited anywhere in the body, and the complex must be eliminated unchanged from the body. Beside commonly used radioisotopes, as isotopes of technetium, iodine and fluorine, metal radioisotopes are increasingly used due to some advantages in their physical and chemical properties. Among them, copper radioisotopes (e.g. ^{64}Cu and ^{67}Cu) exhibit a great potential for both diagnosis (positron emission) and therapy (β^- particles of an intermediate energy).[14–16] Therefore, research focused on new ligands and their copper(II) complexes having suitable properties is a vital part of coordination chemistry. For utilization in nuclear medicine, the complexes must be thermodynamically stable, and complexation by the ligands should be as selective as possible in a class of competing metal ions [e.g. Cu^{II} vs. mainly Zn^{II}, Ca^{II} and Mg^{II}]. However, it is now commonly recognized that kinetic inertness to dissociation of such complexes is more important and is usually decisive for stability in vivo. In addition, a very fast complexation of short-living radioisotopes is required. Substituents on the ligand backbone can also significantly modify other in vivo properties such as bio-distribution of the complexes themselves. Complexes of bifunctional ligands can be conjugated to biological vectors for targeted utilizations.

From the viewpoint of thermodynamic stability and dissociation inertness, the macrocyclic ligands are superior to open-chain chelators. Macrocyclic ligands are often derivatives or analogues of two parent compounds, H_4dota and H_4teta, which are derived from well-known cyclic amines, 1,4,7,10-tetraazacyclododecane (cyclen), and 1,4,8,11-tetraazacyclotetradecane (cyclam), Scheme 1. The H_4dota-like ligands are mostly non-selective; so, they strongly bind all metal ions but preferably lanthanide(III)

[a] Department of Chemistry, Masarykova Universita (Masaryk University),
Kotlářská 2, 61137 Brno, Czech Republic
Fax: +420-54949-2494
E-mail: lubal@chem.muni.cz
[b] Institute of Analytical Chemistry, Academy of Science of the Czech Republic,
Veveří 97, 61142 Brno, Czech Republic
[c] Department of Inorganic Chemistry, Universita Karlova (Charles University),
Hlavova 2030, 12840 Prague 2, Czech Republic
Fax: +420-22195-1253
E-mail: modrej@natur.cuni.cz
Supporting information for this article is available on the WWW under http://dx.doi.org/10.1002/ejic.200900358.

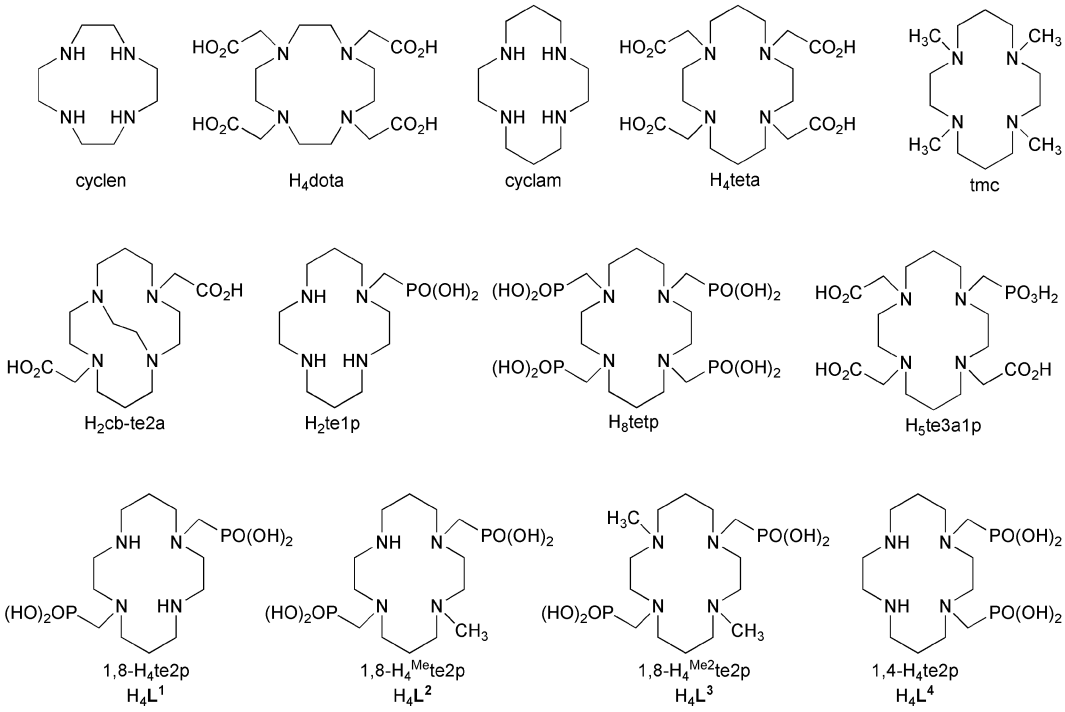

Scheme 1. Structures of ligands mentioned in the text.

or other metal ions requiring high coordination numbers. The cyclam-based ligands such as H_4teta are more appropriate for transition-metal ions as the larger ring allows a planar coordination of all nitrogen atoms.[3,17] However, H_4dota and H_4teta as octadentate ligands usually do not utilize all donor atoms for binding to transition-metal ions in mononuclear species and can form polynuclear complexes. In the case of their copper(II) complexes, it was shown that H_4teta derivatives are not (after conjugation to oligopeptides or antibodies) fully suitable for in vivo applications.[18] Unlike the open-chain ligands, most of the macrocyclic chelators exhibit inconveniently slow kinetics of complex formation; however, a faster complexation rate can be introduced by the design of new macrocyclic ligands.

In the last few years, the research effort has led to some new ligand classes suitable for copper(II) with the view of utilization in nuclear medicine. Among them, the most successful ligands are carboxylate derivatives of so-called "cross-bridged" cyclen and cyclam (e.g. H_2cb-te2a, Scheme 1).[16,19] Their copper(II) complexes are kinetically extraordinarily inert, and their stability in vivo is much higher than that of complexes of other ligands like H_4teta.[19] Beside acetate derivatives, their amides[20] and analogous propionates[21] have been also investigated, and the research has led to a better understanding of the structure–property relationships in this class of ligands. The ligands have been conjugated to some biomolecules, and the conjugates showed good in vivo properties.[22] The main drawback of the cross-bridged ligands is a very slow complexation rate leading to the necessity to use heating and/or non-aqueous solvents for the complexation reactions.[16,19]

Some time ago, we started investigations of cyclam-based ligands containing one or two phosphorus acid arms, which are suitable for the first-row transition-metal ions. Because of strong complexing ability, the phosphonic acid group(s) seem(s) to accelerate the complex formation as (in the case of macrocyclic ligands) the complexation starts with binding of the pendant arms to a metal ion. We synthesized a series of 1,8-bis(phosphonic acid) derivatives of cyclam, having just six coordinating sites.[23] We have studied the *cis*-O,O and *trans*-O,O isomers of nickel(II)[24] and cobalt(III)[25] complexes of 1,8-H_4te2p (Scheme 1); for example we isolated several differently protonated forms, even $[Ni(H_4\mathbf{L^1})]^{2+}$, where the phosphonic acid groups are fully protonated and are coordinated only through the phosphoryl oxygen atom proving a high inertness of the complex against proton-assisted decomplexation. Such coordination was observed for the first time in the solid state. With copper(II), two highly stable isomeric forms of $[Cu(H_2\mathbf{L^1})]$ were isolated.[26] The low-temperature kinetic isomer is pentacoordinate (*pc* isomer) with one phosphonic acid pendant arm non-coordinated and cyclam ring in the conformation **I** (according to Bosnich's nomenclature[27]). On heating, it isomerizes to the thermodynamic octahedral isomer with *trans* arrangement of phosphonic acid moieties and *trans*-**III**[27] cyclam ring conformation. Both isomers are kinetically inert, and the slow acid-assisted decomposition may be a consequence of an overall positive charge of complex species upon the full protonation of non-coordinated phosphonate oxygen atoms.[26] Among divalent metal ions, copper(II) is preferably complexed from thermodynamic as well as kinetic points of view.[28] We also showed that the complex-

ation selectivity can be employed for an efficient analytical determination of copper.[29,30] The main advantage of the ligand is an immediate complex formation (to the *pc* isomer) at pH > 4 and room temperature.[26] The isomeric ligand, 1,4-H_4te2p (H_4**L**^{4}, Scheme 1),[31] forms also very stable complexes and is even more selective for copper(II); an analogous isomerism was observed for the complexes.[32] Similarly, the monophosphonic acid cyclam derivative H_2te1p (Scheme 1) forms a thermodynamically highly stable complex with copper(II) having a cyclam ring in the *trans*-**III** conformation and the phosphonic acid group in the apical position; the complex is also kinetically inert.[33]

It is known that cyclam derivatives fully substituted on the nitrogen atoms (so, only tertiary amines are present, e.g. Me_4cyclam = tmc, Scheme 1) have sometimes very different properties from those of cyclams having one or more secondary amines. Among ligands having six donor atoms, the 4,11-dimethylcyclam derivatives with two coordinating pendant arms in the 1,8-position were mostly studied.[34–37] Complexes of such ligands are often present in conformation **I** of the cyclam ring, and their isomerization to the *trans*-**III** form is rather problematic.[38]

For comparative purposes, we decided to study the coordinating properties of a 4,11-dimethylcyclam-based ligand with two phosphonate pedant arms, 1,8-$H_4{}^{Me2}$te2p (H_4**L**^{3}, Scheme 1). In this paper, we report on the detailed investigation of complexes of this title ligand.

Results and Discussion

Synthesis

In addition to a standard Mannich-type reaction of 1,8-dimethylcyclam with diethyl phosphite and paraformaldehyde in anhydrous benzene,[23] or the analogous reaction of 1,8-dimethylcyclam and paraformaldehyde in neat triethyl phosphite, a novel approach employing direct reaction of a key quarternary intermediate **1** with the sodium salt of diethyl phosphite afforded pure tetraester **2** in quantitative yield. Further hydrolysis in HCl led to the title ligand in overall quantitative isolated yield (Scheme 2). The choice of the solvent in the first step reaction is crucial. If the reaction was performed in neat diethyl phosphite or in less polar solvents (thf, dioxane, toluene), it proceeded with low (< 60%) and non-reproducible yields due to a low solubility of the starting quarternary salt in these solvents. However, in dry dmf the reaction was very fast, and it took only a few minutes until full dissolution of the starting compound.

Crystal Structures

Crystal Structure of (H_6L^3)Cl_2·$4H_2O$

The solid-state structure of the $(H_6\mathbf{L}^3)^{2+}$ cation is one of the rare examples of protonated species among macrocyclic polyaminopolyphosphonic acids and proves a strong acid nature of the aminomethylphosphonic acids as both groups are only single-protonated in the presence of the strong mineral acid. In the structure of $(H_6\mathbf{L}^3)Cl_2{\cdot}4H_2O$, the structurally independent unit is formed by one half of the ligand molecule, one chloride anion and two solvate water molecules. Both independent amino groups are protonated, as well as the phosphonate pendant arm. The macrocyclic skeleton of the hexaprotonated cation $(H_6\mathbf{L}^3)^{2+}$ is in the most common rectangular conformation (3,4,3,4)-A with all amino groups laying in the corners of the rectangle (Figure 1).[1] The same ring conformation has been recently observed for a cation of a monophosphonic acid analogue of H_4teta, $(H_7te3a1p)^{2+}$ (Scheme 1).[39] Each monoprotonated phosphonate group is roughly tetrahedral, with a noticeably longer P–O bond to the proton-bearing oxygen atom (O1, d_{P-O} = 1.57 Å) compared to the unprotonated ones (1.48

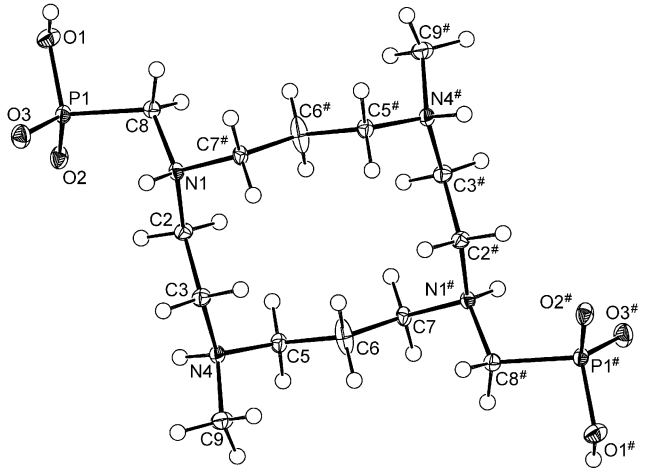

Figure 1. Structure of centrosymmetric molecular cation $(H_6\mathbf{L}^3)^{2+}$ found in the structure of $(H_6\mathbf{L}^3)Cl_2{\cdot}4H_2O$. Thermal ellipsoids show 60% probability level.

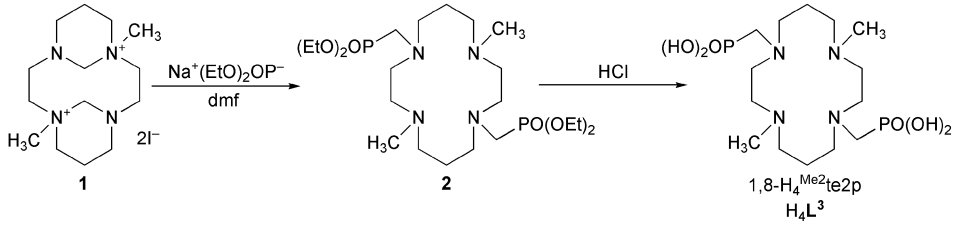

Scheme 2. Novel approach in ligand synthesis.

and 1.51 Å). The whole structure is stabilized by an intermolecular hydrogen-bond system involving strong interactions between protonated amino groups and phosphoryl oxygen atoms of the neighbouring ligand molecules ($d_{N\cdots O}$ = 2.62 and 2.63 Å), and between protonated phosphonate and water solvate molecules ($d_{O\cdots O}$ = 2.59 Å). The chloride anion is involved in medium-strong hydrogen bonds with solvate water molecules ($d_{O\cdots Cl} \approx 3.1$ Å). There are also mutual medium-strong contacts between solvate water molecules, and between the water molecule and the phosphoryl oxygen atom.

Crystal Structure of [Cu(H$_3$L^3)][Cu(H$_2$L^3)]PF$_6$·3H$_2$O

In the structure of [Cu(H$_3$**L**^{3})][Cu(H$_2$**L**^{3})]PF$_6$·3H$_2$O, both structurally independent complex molecules are in a different protonation state. The first complex molecule is triprotonated, once on the coordinated and twice on the non-coordinated phosphonate pendant arms, having an overall charge of 1+; such a protonation results from a low pH value of the mother solution (≈ 2). The second complex unit is diprotonated, once on each of the phosphonate groups (Figure 2), and is electroneutral. The structures of both units are very similar, as can be seen from Figure 2 and from the list of selected geometrical parameters given in Table 1. The space group of the crystal is non-centrosymmetric, and as both independent molecules have also the same chiral configuration (Figure 2), it leads to the presence of only one optically pure species in the crystal. However, both antipodes must be principally formed during a complexation reaction, as there was no source of chirality in the reaction mixture. Therefore, the separation of the optically pure complex is the result of the crystal packing and proceeds spontaneously.

The coordination sphere of the central copper(II) ions is intermediate between square-pyramidal (with an N_4 base) and trigonal-bipyramidal (with N1 and N8 atoms in the apical positions). According to the well-established structural parameter τ, which should be equal to one for the ideal trigonal bipyramid and zero for the ideal square pyramid,[40] the conformation of the complex molecules is a bit closer to the square pyramid (τ = 0.48 and 0.43 for the molecules 1 and 2, respectively). The analogous conformation was observed also for pentacoordinate complexes with non-methylated and monomethylated $(H_2\mathbf{L^1})^{2-}$ and $(H_2\mathbf{L^2})^{2-}$ ligand anions.[26] All N–Cu coordination bonds have an expected length ca. 2.1 Å (Table 1), similar to those observed for coordination of the tertiary amino groups in the copper(II) complexes with $(H_2\mathbf{L^1})^{2-}$ and $(H_2\mathbf{L^2})^{2-}$ anions.[26] Contrary to these structures, the O–Cu coordination bond is slightly shorter (≈ 2.11 and 2.14 Å for both independent units, respectively, see Table 1) compared to the complexes

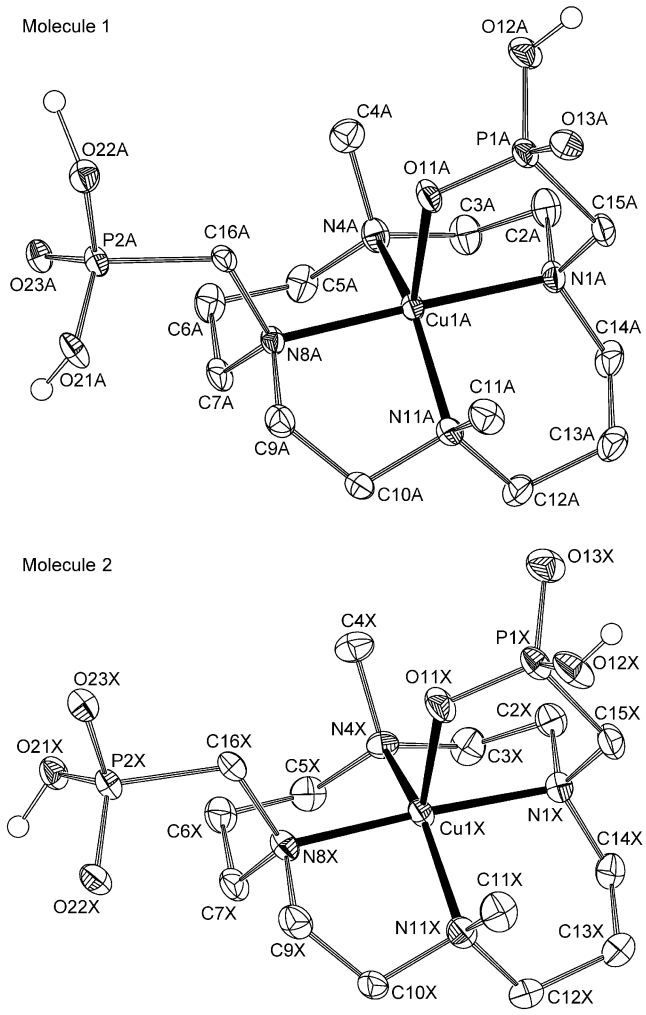

Figure 2. Structure of complex units, [Cu(H$_3$**L**^{3})]$^+$ (molecule 1) and [Cu(H$_2$**L**^{3})] (molecule 2), found in the structure of [Cu(H$_3$**L**^{3})][Cu(H$_2$**L**^{3})]PF$_6$·3H$_2$O. The hydrogen atoms attached to the carbon atoms are omitted for the sake of clarity. Thermal ellipsoids show 60% probability level.

Table 1. Selected geometrical parameters of the complex units found in the structure of [Cu(H$_3$**L**^{3})][Cu(H$_2$**L**^{3})]PF$_6$·3H$_2$O.

Bond [Å]	Molecule 1	Molecule 2	Angle [°]	Molecule 1	Molecule 2
Cu1–N1	2.101(2)	2.109(3)	N1–Cu1–N4	85.91(9)	85.81(10)
Cu1–N4	2.101(3)	2.078(2)	N1–Cu1–N8	178.44(10)	176.97(10)
Cu1–N8	2.093(2)	2.097(2)	N1–Cu1–N11	92.75(10)	91.37(10)
Cu1–N11	2.072(2)	2.088(2)	N1–Cu1–O11	85.11(8)	86.55(9)
Cu1–O11	2.137(2)	2.105(2)	N4–Cu1–N8	93.91(9)	94.67(10)
			N4–Cu1–N11	149.49(10)	151.43(10)
			N4–Cu1–O11	103.64(9)	104.31(9)
			N8–Cu1–N11	86.63(9)	86.78(9)
			N8–Cu1–O11	96.43(8)	96.22(9)
			N11–Cu1–O11	106.62(9)	103.89(10)

with $(H_2\mathbf{L^1})^{2-}$ and $(H_2\mathbf{L^2})^{2-}$ anions (≈ 2.22 and 2.23 Å, respectively). However, the bond angles are very similar in all three structures.

The structure is stabilized by an extensive system of strong intermolecular hydrogen bonds between protonated phosphonates and phosphoryl oxygen atoms of the neighbouring complex molecules ($d_{O\cdots O}$ = 2.45–2.63 Å). There are also medium to strong hydrogen bonds between solvate water molecules, and between the water molecules and the phosphoryl oxygen atoms.

The analogous "overprotonated" species have been also observed in complexes isolated from the Cu^{II}–H_2te1p[33] and Ni^{II}–1,8-H_4te2p[24] systems. This confirms a coordinating ability of the phosphoryl group and a kinetic inertness of such species against acid-assisted decomplexation.

Thermodynamic Properties

The ligand $H_4\mathbf{L^3}$ ($\log\beta_4$ = 37.16) has somewhat lower overall basicity than $H_4\mathbf{L^1}$ ($\log\beta_4$ = 38.55), mostly due to the difference in values of the last two dissociation (first two protonation) constants (Table 2).[23] The reverse order of basic protonation constants is caused by the fact that the concentrations of both $(\mathbf{L^3})^{4-}$ and $(H_2\mathbf{L^3})^{2-}$ species are higher than that of the $(H\mathbf{L^3})^{3-}$ species (see Figure S1). It was shown that these first two protons are bound to ring nitrogen atoms non-bearing pendant phosphonate moieties (i.e. methylated amino groups in the case of $H_4\mathbf{L^3}$ and more basic secondary amino groups in the case of $H_4\mathbf{L^1}$), and the diprotonated species $(H_2\mathbf{L^{1,3}})^{2-}$ are stabilized by strong intramolecular hydrogen bonds between the protonated amino groups and the phosphonate groups.[23] When one proton is dissociated from the diprotonated species forming $(H\mathbf{L^{1,3}})^{3-}$ species, the intramolecular hydrogen-bond system is disrupted, and splitting of the last proton is easier (and occurs formally with lower pK_A). Diprotonated forms of both phosphonate ligands are more basic than tmc or H_4teta, and have comparable basicity to cyclam itself and the tetrakis(phosphonic acid) derivative, H_8tetp (Scheme 1). Going from the alkaline solution, the $(H_2\mathbf{L^3})^{2-}$ species is further protonated in the neutral region to $(H_3\mathbf{L^3})^{-}$ and $H_4\mathbf{L^3}$. In these species, the protonations occur on each phosphonate pendant arm, and the corresponding pK_A values are fully comparable with the values observed for other phosphonates. In the acid region, further protons are attached to remaining nitrogen atoms and/or to the phosphonate groups.

For such systems, thermodynamic stability generally correlates with overall basicity of the ligands[41] and, thus, lower stability constants are expected for complexes of $H_4\mathbf{L^3}$ compared with those of $H_4\mathbf{L^1}$. Stability constants of the title ligand complexes are compiled in Table 3 and their comparison with related systems is given in Table 5. The stabilities of the complexes follow the expected Irving–Williams order of stability of the metal complexes; however, the increase in stability of copper(II) complexes is very high compared to complexes of neighbouring zinc(II) and nickel(II) ions due to an optimal size of the cyclam skeleton for the complexation of the copper(II) ion. Although the stability constants of $H_4\mathbf{L^3}$ complexes are lower than those of $H_4\mathbf{L^1}$, the complexes with transition-metal ions are fully formed in slightly acidic or neutral solutions as can be seen from distribution diagrams in Figure 3 and in the Supporting Information (Figures S2 and S3).

Solution structures of the complexes of $H_4\mathbf{L^3}$ formed in the titrations should be analogous to those observed for complexes of $H_4\mathbf{L^1}$, i.e. corresponding to the low-temperature kinetic isomers.[24–26,28] In the $[M(\mathbf{L^3})]^{2-}$ species, the divalent metal ions [except copper(II), see below] should be coordinated by four nitrogen atoms of the ring and one oxygen atom of each phosphonate group in the octahedral environment. The structure of the protonated species depends on affinity of the particular metal ion for nitrogen or oxygen donor atoms.[28] As dissociation constants of the $[M(H_x\mathbf{L^3})]^{x-2}$ species with first-row transition-metal ions (Table 4) are very similar or lower than phosphonate pK_A

Table 2. Comparison of dissociation constants (pK_A) of $H_4\mathbf{L^3}$ and related ligands.

Equilibrium[a]	$H_4\mathbf{L^3}$[23]	$H_4\mathbf{L^1}$[23]	Cyclam[42]	tmc[43]	H_4teta[44]	H_8tetp[45]
$HL \rightleftharpoons H^+ + L$	11.47	–	11.29	9.36	10.58	–
$H_2L \rightleftharpoons H^+ + HL$	12.17	*26.41* [b]	10.19	9.02	10.17	*25.28*[b]
$H_3L \rightleftharpoons H^+ + H_2L$	7.198	6.78	1.61	2.54	4.09	8.85
$H_4L \rightleftharpoons H^+ + H_3L$	6.326	5.36	1.91	2.25	3.35	7.68
$H_5L \rightleftharpoons H^+ + H_4L$	1.52	1.15	–	–	–	6.23
$H_6L \rightleftharpoons H^+ + H_5L$	–	–	–	–	–	5.33

[a] Charges of species are omitted for reasons of clarity . [b] Numbers in *italics* correspond to a value for a simultaneous dissociation of two protons.

Table 3. Stability constants (β_{hlm})[a] of the metal complexes with $H_4\mathbf{L^3}$.

Equilibrium	Ca^{2+}	Co^{2+}	Ni^{2+}	Cu^{2+}	Zn^{2+}	Cd^{2+}	Pb^{2+}
$M^{2+} + (\mathbf{L^3})^{4-} \rightleftharpoons [M(\mathbf{L^3})]^{2-}$	3.98(8)	15.66(4)	15.55(6)	24.03(9)	17.56(3)	15.89(7)	12.79(3)
$M^{2+} + (\mathbf{L^3})^{4-} + H^+ \rightleftharpoons [M(H\mathbf{L^3})]^{-}$	14.4(3)	22.74(2)	22.82(2)	30.92(5)	24.57(1)	23.03(8)	20.69(3)
$M^{2+} + (\mathbf{L^3})^{4-} + 2\ H^+ \rightleftharpoons [M(H_2\mathbf{L^3})]$	25.61(7)	27.3(4)	27.9(1)	35.97(2)	28.8(1)	29.68(4)	27.51(3)
$M^{2+} + (\mathbf{L^3})^{4-} + 3\ H^+ \rightleftharpoons [M(H_3\mathbf{L^3})]^{+}$	32.3(2)	–	–	–	–	–	33.1(2)

[a] $\beta_{hlm} = [H_hL_lM_m]/\{[H]^h \times [L]^l \times [M]^m\}$.

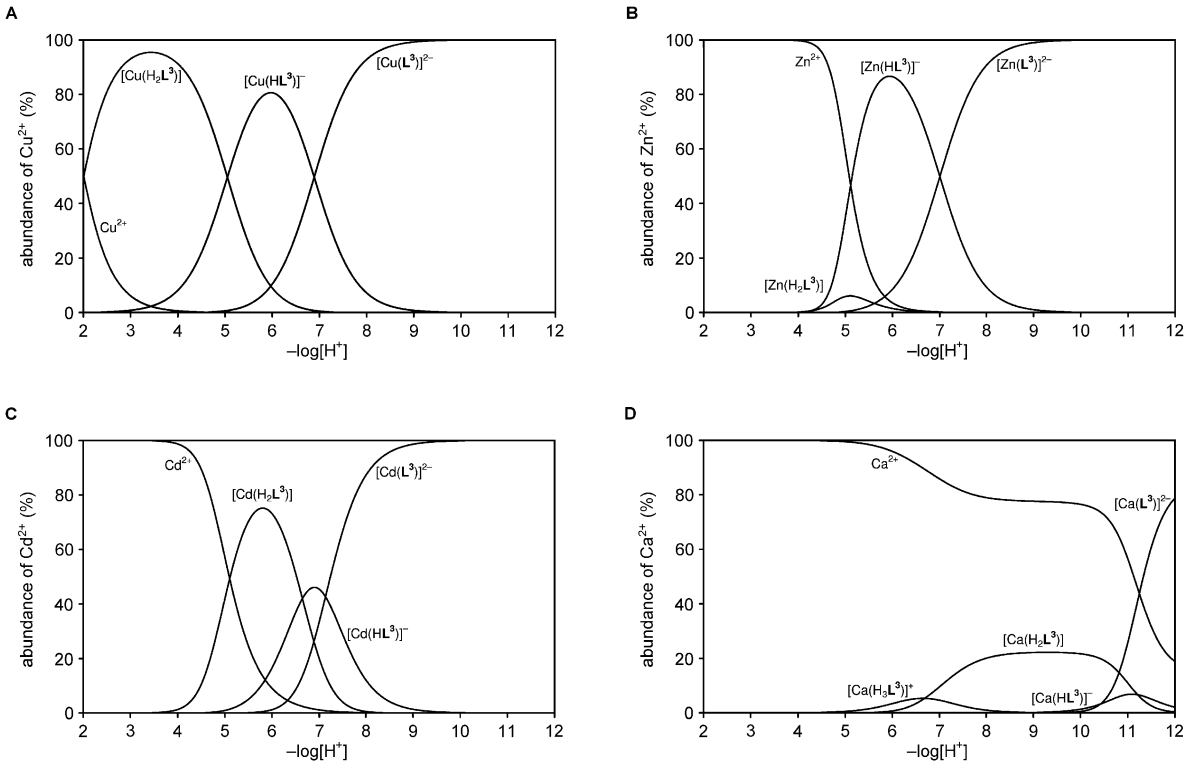

Figure 3. Distribution diagrams of metal-containing species in the M^{II}–$H_4\mathbf{L^3}$ systems with $c_L = c_M = 0.004$ M for $M^{II} = Cu^{II}$ (**A**), Zn^{II} (**B**) and Cd^{II} (**C**) and Ca^{II} (**D**).

values of the ligand (7.2 and 6.3, Table 2), these complex species should be protonated on phosphonate pendant arms. For the corresponding complexes of calcium(II) and lead(II) with higher pK_A values and more (tri)protonated species (Table 4), proton(s) in the protonated species should be also bound on nitrogen atoms of the ring; this is supported by the solid-state structure of the [Pb($H_2\mathbf{L^1}$)] species isolated from a slightly acidic solution.[28] These complexes are formed only after at least a partial deprotonation of the phosphonate pendant arms. In the case of the Ca^{II}–$H_4\mathbf{L^3}$ system, the reverse order of pK_A values of [Ca($H_2\mathbf{L^3}$)] and [Ca($H\mathbf{L^3}$)]$^-$ was observed, as a result of easier (metal-assisted) deprotonation of [Ca($H\mathbf{L^3}$)]$^-$ species. The mechanism of this effect can be viewed as upon deprotonation of [Ca($H_2\mathbf{L^3}$)] species the metal ion moves closer to the macrocyclic cavity and it is (probably) coordinated by part of the macrocycle; therefore, the dissociation of the remaining protonated amino group is strongly preferable due to electrostatic repulsion, and occurs more easily compared to the previous deprotonation. The pK_A values of cadmium(II) complexes lay between these two limits. Therefore, one can expect that there can be some equilibrium between protonated phosphonate arm(s) and macrocycle nitrogen atom(s) in the [Cd($H_2\mathbf{L^3}$)] species; such a conclusion can be supported by a much lower pK_A of the phosphonate found in the kinetic experiments (vide infra). The stability of the magnesium(II) complex is too low to be determined by the method used. The copper(II) species is pentacoordinate analogously as it was found in the solid state (vide supra). The first proton should be bound to the non-coordinated arm and the second one to the coordinated phosphonate group.[26] Examples of the distribution diagrams are shown in Figure 3 [Cu^{II}–, Zn^{II}–, Cd^{II}– and Ca^{II}–$H_4\mathbf{L^3}$ systems] and in the Supporting Information [Figures S2 and S3; Co^{II}– and Ni^{II}–$H_4\mathbf{L^3}$ systems].

Table 4. Dissociation constants [p$K_{A(hlm)}$][a] of the metal complexes with $H_4\mathbf{L^3}$.

Equilibrium	Ca^{2+}	Co^{2+}	Ni^{2+}	Cu^{2+}	Zn^{2+}	Cd^{2+}	Pb^{2+}
$[M(H\mathbf{L^3})]^- \rightleftharpoons [M(\mathbf{L^3})]^{2-} + H^+$	10.4	7.08	7.27	6.89	7.01	7.14	7.90
$[M(H_2\mathbf{L^3})] \rightleftharpoons [M(H\mathbf{L^3})]^- + H^+$	11.21	4.6	5.1	5.05	4.2	6.65	6.82
$[M(H_3\mathbf{L^3})]^+ \rightleftharpoons [M(H_2\mathbf{L^3})] + H^+$	6.7	–	–	–	–	–	5.6

[a] $pK_{A(hlm)} = \log\beta_{hlm} - \log\beta_{(h-1)lm}$.

Complexes of $H_4\mathbf{L^3}$ are much more stable than those of tmc (Scheme 1) for all the metal ions investigated due to the presence of additional binding groups (forming additional chelate rings) and the higher overall ligand basicity (Table 5). The very high stabilities of the copper(II) complexes observed for the ligands confirm the good fit of the cyclam ring for this metal ion. However, the newly studied ligand $H_4\mathbf{L^3}$ is more selective for copper(II) complexation than was observed for $H_4\mathbf{L^1}$ and for the commonly used H_4teta; the thermodynamic selectivity is similar to that of tmc. By comparing the distribution diagrams shown in Figure 3, it can be seen that the copper(II) ion is fully com-

Table 5. Comparison of stability constants (β_{011}) of complexes of $H_4\mathbf{L^3}$ and related ligands.

Cation	$H_4\mathbf{L^3}$	$H_4\mathbf{L^1}$[26,28]	Cyclam[43]	tmc[43]	H_4teta[43,44b]	H_8tetp[45,46]
Ca^{2+}	3.98	5.26	–	–	8.42	–
Co^{2+}	15.66	19.28	–	7.58	16.6	–
Ni^{2+}	15.55	21.99	22.2	8.65	19.91	–
Cu^{2+}	24.03 (*pc*)[a]	25.40 (*pc*),[a] 26.50 (*trans*)[b]	28.1	18.3	21.74	25.99
Zn^{2+}	17.56	20.35	15.2	10.4	16.62	17.6
Cd^{2+}	15.89	17.89	11.3	9.0	18.25	16.7
Pb^{2+}	12.79	14.96	10.9	–	14.3	15.5

[a] *pc* means kinetic pentacoordinate species. [b] *trans* means thermodynamic *trans*-O,O-octahedral species.

plexed below $-\log[H^+] \approx 4$, where zinc(II) or cadmium(II) ions just start to be complexed; so, pH ≈ 4 is suitable for a fully selective formation of the copper(II)–$H_4\mathbf{L^3}$ complex.

Formation Kinetics

As the rate of complexation is a central point for any possible radiopharmaceutical applications, the formation kinetics for copper(II), zinc(II) and cadmium(II) complexes were studied. The formation of the copper(II) complex was monitored directly. The indirect indicator method (commonly employed in the chemistry of macrocyclic ligands[47]) was used to visualize a course of the reactions as there is no UV/Vis absorbing group or species in the Zn^{II}–$H_4\mathbf{L^3}$ or Cd^{II}–$H_4\mathbf{L^3}$ systems; however, this leads to somewhat less precise results compared with conventional direct methods.[48] At pH higher than ca. 5, the stopped-flow technique was employed as the complexation reactions were noticeably faster.

At the first stage, it was proved that the collected data correspond to a first-order process with respect to the metal ion; it was found that the dependence of the observed pseudo-first-order rate constant ${}^{fM}k_{obs}$ (measured at constant pH) is a linear function of the metal ion concentration, i.e. ${}^{fM}k_{obs} = {}^{fM}k_2 \times [M^{2+}]$, giving a slope of logarithmic analysis equal to one. Examples of such experimental data are shown in the Supporting Information (Figure S4). Therefore, the presence of complexes with higher metal/ligand ratio (e.g. M_2L) in the mechanism can be excluded.

According to the distribution diagram of the free ligand, three differently protonated species (see Experimental Section and Figure S1) are present in solution in the investigated pH range. In principle, each of these ligand species can take part in the complexation reaction with the metal ions to form the final $[M(H_n\mathbf{L^3})]^{n-2}$ (n = 0–2) complexes. A generally accepted mechanism of complex formation (relevant for the M^{II}–$H_4\mathbf{L^3}$ systems) is shown in Scheme 3. The constants K_3 and K_4 are particular consecutive protonation constants of the corresponding ligand species $(H_2\mathbf{L^3})^{2-}$ and $(H_3\mathbf{L^3})^-$ {see Table 2, e.g. $\log K_3 = pK_A[(H_3\mathbf{L^3})^-]$}, and K_{211} and K_{111} are protonation constants of the $[M(H\mathbf{L^3})]^-$ and $[M(\mathbf{L^3})]^{2-}$ complexes, respectively {see Table 4, e.g. $\log K_{211} = pK_A[M(H_2\mathbf{L^3})]$}. From this general scheme, the dependence of the second-order formation constant ${}^{fM}k_2$ on proton concentration can be derived as given by Equation (1) [for details of evaluation of Equation (1), see Supporting Information].

$$ {}^{fM}k_2 = \frac{{}^{fM}k_{H_2L} + {}^{fM}k_{H_3L} \times K_3 \times [H^+] + {}^{fM}k_{H_4L} \times K_3 \times K_4 \times [H^+]^2}{1 + K_3 \times [H^+] + K_3 \times K_4 \times [H^+]^2} \quad (1) $$

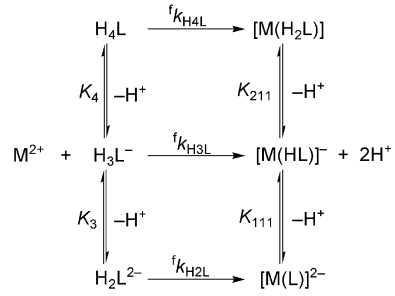

Scheme 3. General mechanism of complex formation.

The obtained second-order formation rate constants ${}^{fM}k_2$ (calculated from the observed rate constant ${}^{fM}k_{obs}$ by ${}^{fM}k_2 = {}^{fM}k_{obs}/[M^{2+}]$) were treated as a function of proton concentration [according to Equation (1)], by testing various kinetic models with a set of partial rate constants (corresponding to the reactivity of the differently protonated ligand species) in order to obtain the best fit for the experimental data. However, involvement of only some protonated species led to a good fit, and corresponding constants for the protonated ligand species are given for Cu^{II} in Table 6 and for Cd^{II} in Table 8. The best fitting results {modified by involvement of the $[Zn(OH)]^+$ species, see below} are shown in Figure 4.

In the case of the zinc(II) complexation, the fit according to Equation (1) was in good agreement with the experimental data only at pH < 5; the acceleration at pH > 5.5 could not be successfully described by Equation (1). Therefore, an additional reaction pathway had to be taken into account. The acceleration can be attributed to the reaction of the monohydroxido $[Zn(OH)]^+$ species as, in general, hydroxido species are more reactive than aqua ions,[48] although their concentration is very low {at given pH range, the abundance of $[Zn(OH)]^+$ in the Zn^{2+}–OH^- system reaches 0.1–0.8%}. Therefore, Scheme 3 should be modified by in-

Table 6. Second-order formation rate constants ^{fCu}k ($mol^{-1}\,dm^3\,s^{-1}$) for the reaction of Cu^{II} ions with $H_4\mathbf{L^3}$ and similar ligands (25 °C).

Ligand	$^{fCu}k_{H_4L}$	$^{fCu}k_{H_3L}$	$^{fCu}k_{H_2L}$	$^{fCu}k_{HL}$	$^{fCu}k_{OH}$
$H_4\mathbf{L^3}$	0.04(2)	$2.8(4)\times10^3$	$2.8(6)\times10^6$	–	–
$H_4\mathbf{L^1}$[26]	0.17	1.38×10^3	1.97×10^5	–	–
cyclam	–	–	0.135 (ref.[53]) 0.39 (ref.[54]) 0.076 (ref.[52])	1.05×10^6 (ref.[53]) 1.8×10^6 (ref.[54]) 8.0×10^6 (ref.[52]) 2.6×10^5 (ref.[50])	–
1-Mecyclam[50]	–	–	–	1.2×10^7	–
1,11-Me_2cyclam[50]	–	–	–	2.8×10^6	–
tmc[50]	–	–	–	2.9×10^5	–
5,12-Me_2cyclam[55]	–	–	9.1×10^2	6.44×10^5	1.17×10^7
cyclen	–	–	0.6 (ref.[54]); 0.180 (ref.[56])	2.9×10^6 (ref.[54]); 1.84×10^6 (ref.[56])	–
H_4dota[47]	–	–	5×10^3	1.2×10^9	–

Table 7. Second-order formation rate constants ^{fZn}k ($mol^{-1}\,dm^3\,s^{-1}$) for the reaction of Zn^{II} ions with $H_4\mathbf{L^3}$ and similar ligands (25 °C).

Ligand	$^{fZn}k_{H_4L}$	$^{fZn}k_{H_3L}$	$^{fZn}k_{H_2L}$	$^{fZn}k_{HL}$	$^{fZn}k_{OH}$
$H_4\mathbf{L^3}$	0.30(14)	2(1)	$3(1)\times10^2$	$1.0(1)\times10^{10}$ [a]	$1.1(1)\times10^7$[b]
$H_4\mathbf{L^1}$ [28]	0.16	7.4	3.3×10^2	2.5×10^{10} [a]	1.0×10^5
cyclam	–	–	1.0 (ref.[57])	7.5×10^4 (ref.[57]) 5.0×10^4 (ref.[54])	–
tmc[58]	–	–	–	4.5×10^3	–
5,12-Me_2-cyclam[55]	–	–	1.43×10^5	1.01×10^8	2.40×10^9
H_4teta[47]	–	–	–	1.6×10^8	–
cyclen	–	–	3.9 (ref.[57])	1.3×10^5 (ref.[57]) 3.3×10^4 (ref.[54])	–
H_4dota[47]	–	–	–	1.1×10^7	–

[a] Estimated value for the $[Zn^{2+} + (H\mathbf{L^{1,3}})^{3-}]$ pathway when the "$Zn(OH)^+ + (H_2\mathbf{L^{1,3}})^{2-}$" contributions were neglected [i.e. fit with Equation (S11) (see Supporting Information) with fixed values of other rate constants]. [b] Calculated for fixed values of rate constants $^{fZn}k_{H_4L}$ and $^{fZn}k_{H_3L}$, which were determined from fitting of data at pH < 5.5 (see text).

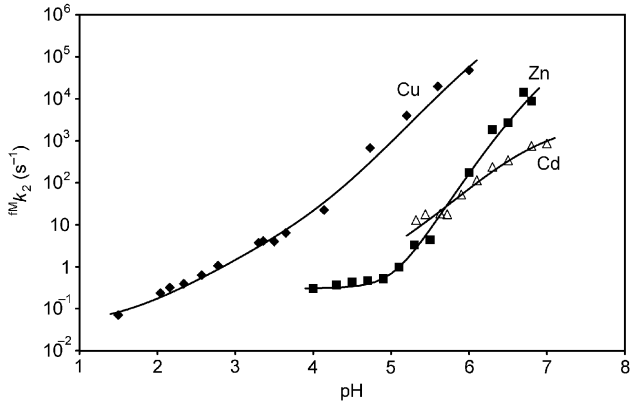

Figure 4. The pH dependence of the second-order rate constant $^{fM}k_2$ for the formation of the $H_4\mathbf{L^3}$ complexes. The curves show the best results of fitting by Equation (1) for (a) Cu^{II} (full diamonds) and (c) Cd^{II} (empty triangles) and (b) fitting by Equation (2) for Zn^{II} (full squares).

clusion of the hydroxido complex pathway (Scheme S1) to give Equation (2) [for details of evaluation of Equation (2), see Supporting Information]. It should be noted that formally the same scheme and equation can be obtained with involvement of the $(H\mathbf{L^3})^{3-}$ species due to a proton ambiguity. However, involvement of the hydroxido species is more suitable as the ligand species $(H_2\mathbf{L^3})^{2-}$ is highly basic (Table 2) and, thus, the concentration of $(H\mathbf{L^3})^{3-}$ in the given pH range is negligible. On the contrary, the abundance of the $[Zn(OH)]^+$ complex is higher than that of the hydroxido species of Cu^{II} and Cd^{II} in the given pH region which clearly explains the increase of the rate of Zn^{II} complexation compared to the other ions [see especially Zn^{II} vs. Cd^{II} in Figure 4]. Furthermore, the participation of (hydroxido)metal species was also suggested in the complexation of other macrocyclic ligands.[28,49] Thus, data for the Zn^{II}–$H_4\mathbf{L^3}$ system (similarly to the Zn^{II}–$H_4\mathbf{L^1}$ system[28]) were treated according to Equation (2), where β_{-101} is the stability constant for formation of the $[Zn(OH)]^+$ species, and the results are compiled in Table 7.

$$^{fZn}k_2 = \frac{^{fZn}k_{OH}\times\beta_{-101} + {}^{fZn}k_{H_2L}\times[H^+] + {}^{fZn}k_{H_3L}\times K_3\times[H^+]^2 + {}^{fZn}k_{H_4L}\times K_3\times K_4\times[H^+]^3}{[H^+] + K_3\times[H^+]^2 + K_3\times K_4\times[H^+]^3} \quad (2)$$

Formation Kinetics of the Copper(II) Complex

The rate of copper(II) complexation is of paramount importance in the design of new ligands for copper isotopes. The data for $H_4\mathbf{L^3}$ and similar ligands are presented in Table 6. Although electroneutral species $H_4\mathbf{L^1}$ and $H_4\mathbf{L^3}$ have low and comparable reactivity, the negatively charged di- and triprotonated forms of the title ligand anion [$(H_2\mathbf{L^3})^{2-}$ and $(H_3\mathbf{L^3})^-$, respectively] are more reactive than the analogously protonated forms of $H_4\mathbf{L^1}$; the corresponding constants for the title ligand are ca. 2 times ($^{fCu}k_{H_3L}$)

or ca. 14 times ($^{fCu}k_{H_2L}$) higher than those for $H_4\mathbf{L^1}$. The difference can be explained by weaker intramolecular hydrogen bonds between phosphonate groups and protonated amino groups in anionic species of the title ligand compared to those of $H_4\mathbf{L^1}$ as a result of lower basicity and/or higher steric hindrances of the methylated macrocycle amino group in $H_4\mathbf{L^3}$ [this difference is even more pronounced in the diprotonated species $(H_2\mathbf{L^3})^{2-}$ and $(H_2\mathbf{L^1})^{2-}$]. For both ligands, such intramolecular hydrogen bonds were found in the solid state as well as proving to be present in solution.[23,28] A similar effect was observed in the case of cyclam and its *N*-methylated derivatives. The presence of one or two methyl groups led to an acceleration by a factor of about 100 and 10 (probably as a result of the less symmetrical and weaker hydrogen-bond interaction between the macrocycle nitrogen atoms), whereas for 1,4,8,11-tetramethylcyclam (tmc) the same reactivity was observed as for cyclam itself (probably for steric reasons).[50]

Reactivity of both diprotonated phosphonate ligands $(H_2\mathbf{L^1})^{2-}$ and $(H_2\mathbf{L^3})^{2-}$ is much higher than those of diprotonated cyclam and cyclen (the diprotonated forms of the ligands are protonated on two ring nitrogen atoms). This clearly shows a rate enhancement brought by the presence of strongly coordinating negatively charged phosphonate pendant arms. An analogous effect was observed in similar systems having a carboxylate substituent as the side group, compared to the non-substituted macrocycle and the analogous amino group derivative.[51] The pendants are involved in the fast formation of an outer-sphere (out-of-cage) complex and assist a rate-limiting (slow) translocation of the metal ion to the macrocyclic cavity with a simultaneous removal of proton(s). Overall, the reactivity of both phosphonate ligands is comparable; a small difference between the observed formation rate constant (slightly faster complexation of the $H_4\mathbf{L^1}$ ligand) can be found in strongly acidic media as a result of a higher stability of the Cu^{II}–$H_4\mathbf{L^1}$ complex in this region (Figure S5). A rate enhancement caused by the presence of coordinating pendant arms was also observed in the case of H_4dota complexation,[47] but it is not so pronounced as in the case of these phosphonate ligands. A similar effect was also observed even when complexation proceeded in the presence of a coordinating (acetate) buffer, which compensates the positive charge of the metal ion by formation of weak acetate complexes and drops overall repulsion between the metal ion and the positively charged protonated macrocyclic backbone.[52]

Because of the slow rate of complexation observed in the case of some ligands, the reaction could be monitored at relatively high pH values, which enable one to determine the rate constant $^{fCu}k_{HL}$ associated with the monoprotonated ligand species pathway. Typically, this rate constant is of similar order of magnitude as the rate constants observed for the diprotonated ligand species of the phosphonate ligands (Table 6), proving again the rate enhancement due to the presence of the strongly coordinating phosphonate pendants.

Formation Kinetics of the Zinc(II) Complex

The efficient increase of reactivity of the ligand to the zinc(II) ion observed at pH > 5.5 can be successfully described by inclusion of the partial reaction $[Zn(OH)]^+ + (H_2\mathbf{L^3})^{2-}$ into the reaction scheme (Scheme S1) and is reflected by a high value of the corresponding partial rate constant $^{fZn}k_{OH}$. However, to keep the low number of fitted parameters for a reasonable estimation of standard errors, the rate constants $^{fZn}k_{H_4L}$, $^{fZn}k_{H_3L}$ and $^{fZn}k_{H_2L}$ were fitted by using data for pH < 5.5. After a successful fit, the values of $^{fZn}k_{H_4L}$ and $^{fZN}k_{H_3L}$ were fixed, and the rate constants $^{fZn}k_{H_2L}$ or $^{fZn}k_{OH}$ were calculated with inclusion of data obtained for pH > 5.5. The increased reactivity of zinc(II) (compared to the other metal ions) towards macrocyclic ligands at higher pH values is normal, and a pathway employing monoprotonated ligand species $[Zn^{2+} + (H\mathbf{L^3})^{3-}]$ has been suggested for several ligands.[54,57] This partial reaction affords formally the same rate law, but different partial rate constants. Therefore, we also fitted the experimental data using Equation (S11), which was derived including this pathway to obtain the corresponding rate constant $^{fZn}k_{HL}$ for comparative purposes. The results are also compiled in Table 7. The tentative value $^{fZn}k_{HL} = 1.0 \times 10^{10}\ mol^{-1}\,dm^3\,s^{-1}$ was obtained, which is of the same order of magnitude as the corresponding constant calculated analogously for the Zn^{II}–$H_4\mathbf{L^1}$ system (Table 7) but much higher than rate constants observed in other systems. Overall, the reactivity of both phosphonate ligands is fully comparable (Figure S6).

Formation Kinetics of the Cadmium(II) Complex

Unfortunately, there is little literature data dealing with Cd^{II} complexation in relevant systems. However, compared to the parent $H_4\mathbf{L^1}$ ligand, it can be seen that the reactivity of the methylated ligand $H_4\mathbf{L^3}$ is noticeably higher than that of $H_4\mathbf{L^1}$, as a consequence of lower basicity of the nitrogen donor groups which enables easier removal of a proton from the macrocyclic rim and accelerates the coordination, and the relatively high stability of the protonated complexes (vide supra) (Table 8, Figure S7).

The enhanced copper(II) selectivity is not demonstrated for the uncharged species H_4L (compare values in Table 6, Table 7 and Table 8) for both bis(phosphonate) ligands

Table 8. Second-order formation rate constants ^{fCd}k ($mol^{-1}\,dm^3\,s^{-1}$) for reaction of Cd^{II} ions with $H_4\mathbf{L^3}$ and similar ligands (25 °C).

Ligand	$^{fCd}k_{H_4L}$	$^{fCd}k_{H_3L}$	$^{fCd}k_{H_2L}$	$^{fCd}k_{HL}$
$H_4\mathbf{L^3}$	–	50(10)	$2.8(3) \times 10^3$	–
$H_4\mathbf{L^1}$[28]	0.15	9.1	1.3×10^2	–
Cyclen[57]	–	–	1.8	3.5×10^5

$H_4\mathbf{L^1}$ and $H_4\mathbf{L^3}$, whereas the charged $(H_3L)^-$ and $(H_2L)^{2-}$ species are responsible for the kinetic selectivity of copper(II) complexation, and it is similar for both ligands. Comparisons of formation rate constants are shown in Figures S5–S7. However, the observed order of formation rates $Cu^{II} >> Cd^{II} > Zn^{II}$ corresponds well with the rate of water exchange in the corresponding (aqua)metal complexes.[59] This fact roughly corresponds with the expected Eigen–Wilkins mechanism.[48,60]

Decomplexation Kinetics

As sufficient kinetic inertness is of main importance for in vivo utilizations, we studied acid-assisted dissociation kinetics for selected complexes to establish particular rate constants of dissociation steps.

Dissociation Kinetics of the Copper(II) Complex

The acid-assisted dissociation kinetics of the copper(II) complex was investigated in 0.1–1.25 M $HClO_4$ and an ionic strength 5 M $(Na,H)ClO_4$ at room and elevated temperatures. The experimental data were successfully fitted by using Equation (3), which corresponds to a commonly accepted mechanism shown in Scheme 4. The best fits are shown in Figure 5. An analogous dissociation mechanism is commonly suggested for dissociation of the macrocyclic complexes and was used for the Cu^{II}–cyclam complex itself.[61] Contrary to this, over-protonation of the reaction intermediates had to be suggested for the related complex of $H_4\mathbf{L^1}$ giving, in the numerator, a polynomial of higher order than that in the denominator.[26] However, this latter type of the rate law had to be used in the case of dissociation of Zn^{II} and Cd^{II} complexes (vide infra).

$$ {}^{dCu}k_{obs} = \frac{{}^{dCu}k \times K_{Cu} \times [H^+]}{1 + K_{Cu} \times [H^+]} \quad (3) $$

The calculated values of the rate constants and the activation parameters are presented in Table 9. The dissociation is associated with a protonation step proceeding with $\log K_{Cu} \approx 1.5$ (Table 9), which corresponds to the first pK_A of the phosphonate group.[24,26] Contrary to this, in the case of the corresponding $H_4\mathbf{L^1}$ complex, the dissociation was preceded by a protonation step with much lower pK_A (≈ 0.3).[26] From these facts, one can conclude that the reactive intermediate of the Cu^{II}–$H_4\mathbf{L^3}$ complex has a lower degree of protonation than that of the analogous Cu^{II}–$H_4\mathbf{L^1}$ complex. However, as the activation parameters of the dissociation step are comparable for both systems (Table S1), the mechanism of dissociation is probably very similar. The only difference is that, in the case of the Cu^{II}–$H_4\mathbf{L^3}$ system, the less protonated complex undergoes a dissociative pathway similar to the analogous Cu^{II}–$H_4\mathbf{L^1}$ system. The much lower inertness of the copper(II) complex with $H_4\mathbf{L^3}$ compared to those of $H_4\mathbf{L^1}$ and cyclam [e.g. half-lives of the corresponding pentacoordinate complexes in 1 M $HClO_4$ and at 25 °C are 19.7 min for the Cu^{II}–$H_4\mathbf{L^1}$ complex[26] and 2.5 min for the Cu^{II}–$H_4\mathbf{L^3}$ complex] can be caused by a more opened structure as the coordination bonds of tertiary amino groups (Cu–N) are longer than those formed by the secondary amino groups and, thus, the transfer of protons from the pendant arm to the macrocycle nitrogen atom can proceed more easily. For visual comparison of the observed dissociation rate constants of the copper(II) complexes of $H_2\mathbf{L^1}$ and $H_2\mathbf{L^3}$, see Figure S8.

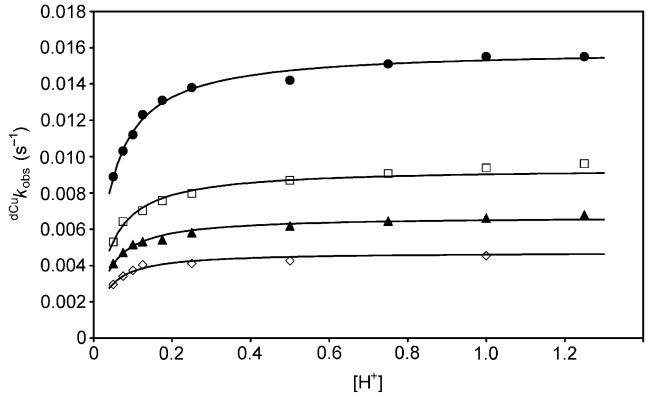

Figure 5. Dependence of the dissociation rate constants of the Cu^{II}–$H_4\mathbf{L^3}$ complex on proton concentration and temperature. 20 °C – open diamonds; 25 °C – full triangles; 30 °C – open squares; 35 °C – full circles. The lines correspond to the best fits according to Equation (3).

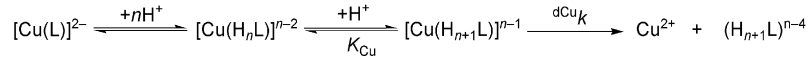

Scheme 4. Reaction mechanism proposed for the dissociation of the Cu^{II}–$H_4\mathbf{L^3}$ complex.

Table 9. Kinetic parameters of acid-assisted dissociation of copper(II) complexes of $H_2\mathbf{L^3}$.

Rate/equilibrium constants	Temperature 293.2 K	298.2 K	303.2 K	308.2 K	Activation/thermodynamics parameters
${}^{dCu}k$ [s^{-1}]	$4.73(15) \times 10^{-3}$	$6.70(9) \times 10^{-3}$	$9.36(16) \times 10^{-3}$	$15.9(2) \times 10^{-3}$	E_a = 60(5) kJ mol^{-1}[a] $\Delta H^{\#}$ = 57(5) kJ mol^{-1} [b] $\Delta S^{\#}$ = –95(18) J K^{-1} mol^{-1}[b]
K_{Cu} [mol^{-1} dm^3]	35(4)	31(2)	26.5(1.6)	25.1(1.0)	ΔH = –17(2) kJ mol^{-1} [c] ΔS = –30(6) J K^{-1} mol^{-1}[c]
$\log(K_{Cu})$	1.54	1.49	1.42	1.40	

[a] Arrhenius model [$\ln k = -(E_a/RT) + \ln A$]. [b] Eyring model [$\ln(k/T) = -(\Delta H^{\#}/RT) + (\Delta S^{\#}/R) + \ln(k_B/h)$]. [c] $\ln K_{Cu} = -(\Delta H/RT) + (\Delta S/R)$.

Dissociation Kinetics of the Zinc(II) and Cadmium(II) Complexes

The dissociation kinetics of the zinc(II) and cadmium(II) complexes was studied in the pH range 3.6–5.9 for the zinc(II) complex and 4.5–6.1 for the cadmium(II) complex. In these regions, the equilibrated systems contain free metal(II) ions as well as the di-, mono- and non-protonated complexes, $[M(H_2\mathbf{L}^3)]$, $[M(H\mathbf{L}^3)]^-$ and $[M(\mathbf{L}^3)]^{2-}$ (see distribution diagrams shown in Figures 3b and c). Only $[M(H_2\mathbf{L}^3)]$ and $[M(H\mathbf{L}^3)]^-$ species are present at high concentrations; the concentrations of fully deprotonated species, $[M(\mathbf{L}^3)]^{2-}$ of both metal(II) complexes, are negligible. One can suppose that, at low pH, further protonation occurs producing thermodynamically unstable species $[M(H_3\mathbf{L}^3)]^+$. Such a protonation should proceed with a constant comparable to those found for analogous protonation of copper(II) ($\log K_{311}$ = 1.21 or 1.52)[26] or nickel(II) ($\log K_{311}$ = 1.15)[24] complexes of $H_4\mathbf{L}^1$. Therefore, the concentration of $[M(H_3\mathbf{L}^3)]^+$ should be also very low in the used pH region. According to these suggestions, a general reaction scheme can be drawn (Scheme 5) giving the dependence of the observed dissociation rate constant on pH expressed by Equation (4). Equation (4) formally corresponds to the equation used for fitting of dissociation data for the *pc*-$[Cu(H_4\mathbf{L}^1)]^{2+}$ complex.[26] Here, the constants K_{111}–K_{311} correspond to the protonation equilibrium of the complexes and should be numerically equal to inverted dissociation constants {i.e. $\log K_{111} = pK_{A(111)}$ and $\log K_{211} = pK_{A(211)}$ from Table 4, and $\log K_{311} = pK_A$ of the triprotonated $[M(H_3\mathbf{L}^3)]^+$ species}.

$$ {}^{dM}k_{obs} = \frac{{}^{dM}k_0 + {}^{dM}k_1 \times K_{211} \times [H^+] + {}^{dM}k_2 \times K_{211} \times K_{311} \times [H^+]^2}{1 + K_{211} \times [H^+]} \quad (4) $$

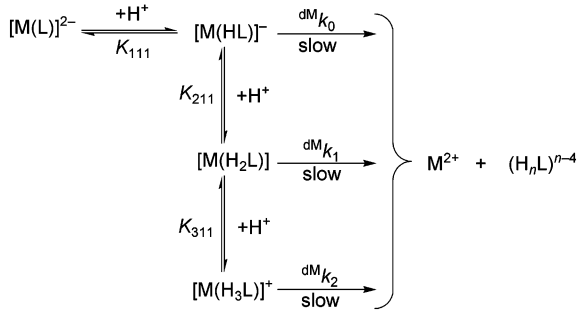

Scheme 5. The reaction mechanism proposed for dissociation of the zinc(II) and cadmium(II) complexes with $H_4\mathbf{L}^3$.

The experimental data of pseudo-first-order rate constants, ${}^{dM}k_{obs}$, for both metal(II) complexes were fitted through the experimental points by using Equation (4). However, as the value of K_{311} can only be estimated on the basis of values reported for Cu^{II}[26] and/or Ni^{II}[24] complexes of $H_4\mathbf{L}^1$, the overall value of product ${}^{dM}k_2 \times K_{311}$ was fitted. In the case of the Zn^{II} complex dissociation, all rate constants can be reliably calculated, and K_{211} was fixed to the value obtained by potentiometry ($10^{4.2}$, Table 4). However, in the case of Cd^{II} complex dissociation, only the value of ${}^{dM}k_2 \times K_{311}$ can be reliably calculated. In addition, the value of K_{211} had to be fitted too, as its fixing to the value obtained by potentiometry ($10^{6.65}$, Table 4) led to a very poor fit. The large discrepancy between the values obtained from the kinetic study ($10^{4.99}$) and potentiometry ($10^{6.65}$) can be attributed to a partial protonation of nitrogen atoms in the equilibrated system (vide supra) which increases the apparent overall pK_A associated with the $[Cd(H_2\mathbf{L}^3)]/[Cd(H\mathbf{L}^3)]^-$ deprotonation. Contrary to this, in the kinetic study, the $[Cd(\mathbf{L}^3)]^{2-}$ complex with the fully encapsulated metal ion was added to acidic media and the protonation is, therefore, associated with the non-coordinated oxygen atoms of the pendant arm(s) as all nitrogen atoms are coordinated to the cadmium(II) ion. The best fits of the experimental data are given in Figure 6 and the resulting values in Table 10.

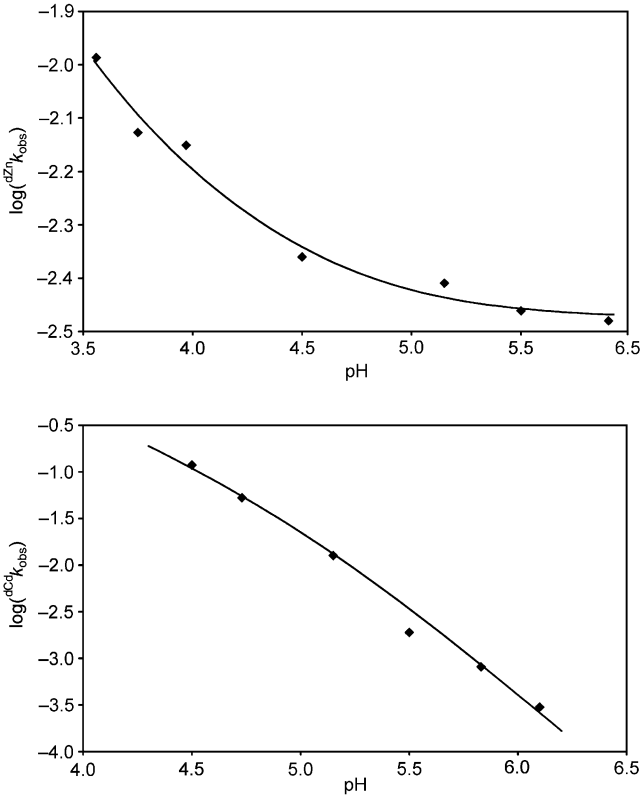

Figure 6. Dependence of dissociation rate constants of zinc(II) and cadmium(II) complexes with $H_4\mathbf{L}^3$ on pH. The curves show the best fits according to Equation (4).

Table 10. Summary of partial dissociation rate constants determined for zinc(II) and cadmium(II) complexes with $H_4\mathbf{L}^3$ and their comparison with complexes of $H_4\mathbf{L}^1$ (25 °C, 0.1 M KCl).

Rate constant	$H_4\mathbf{L}^3$		$H_4\mathbf{L}^1$ (ref.[28])	
	Zn^{II}	Cd^{II}	Zn^{II}	Cd^{II}
${}^{dM}k_0$	$3.3(2)\times10^{-3}$	–	–	–
${}^{dM}k_1$	$6.4(1.0)\times10^{-3}$	–	3×10^{-3}	$<3\times10^{-4}$
${}^{dM}k_2 \times K_{311}$	19(5)	$4.6(5)\times10^3$	18	2.48×10^3

The same order of the corresponding partial rate constants for both related ligands (Table 10) reflects a similar mechanism and closely similar geometry of the complex species. However, the observed dissociation pathway of $[Zn(HL^3)]^-$ species (i.e. $^{dZn}k_0$) leads to a much lower kinetic inertness of this complex at neutral pH (compare $^{dZn}k_{obs}$ of both ligands, see Figure S9). Such a behaviour can be attributed to a higher steric strain of the methyl substituents, which prevents an optimal encapsulation of the metal ion and leads, in the case of the Zn^{II}–H_4L^3 complex, to longer coordination bonds and a more open structure compared to the Zn^{II}–H_4L^1 complex. The dissociation rates of Cd^{II} complexes of both ligands are very similar (Figure S10) and much higher than the rates observed for the corresponding Zn^{II} complexes, as a result of the larger metal ion, not optimally fitting the ligand cavity.

It can be supposed that the logarithm of protonation constant $\log K_{311}$ for all complexes should be about 1–2 and, therefore, the concentration of the triprotonated reaction intermediates is at a trace level under the experimental conditions used in this study. However, the product $^{dM}k_2 \times K_{311}$ is several orders of magnitude larger than $^{dM}k_1$ (and it is more pronounced for the Cd^{II} complexes compared to the Zn^{II} ones). It reflects a much higher reactivity of the triprotonated species over the diprotonated ones. Such a higher reactivity is probably caused by the fact that the third proton is very easily transferred from the pendant(s) to a ring nitrogen atom leading to a very fast decomposition. Generally, the Zn^{II}–$H_4L^{1,3}$ complexes are kinetically much more inert than the cadmium(II) complexes. This observation is related to the size and conformation of the macrocyclic ring cavity, which accommodates the smaller metal cations such as Cu^{II} or Zn^{II} more easily than the larger ones, e.g. Cd^{II}.

Conclusions

A novel synthetic approach for the introduction of a methylphosphonic acid pendant arm was developed. It is based on the reaction of quarternized cyclam-formaldehyde aminal with a sodium salt of diethyl phosphite. The phosphite anion selectively opens the weak C–N bond of the quarternized amine. The prepared tmc analogue forms thermodynamically stable complexes with transition-metal ions showing very high selectivity for the copper(II) ion. In the solid state, the Cu^{II}–H_4L^3 complex is pentacoordinate with an intermediate arrangement between square-pyramidal and trigonal-bipyramidal (τ = 0.43 and 0.48) and one pendant arm non-coordinated. Although the Cu^{II}–H_4L^3 complex is kinetically still relatively inert (e.g. half-life in 1 M $HClO_4$ at 25 °C is ca. 2.5 min), it is kinetically much more labile than the copper(II) complexes of the analogous non-methylated bis(phosphonic acid) ligand, H_4L^1 ($\tau_{1/2}$ = 19.7 min for *pc*-Cu^{II}–H_4L^1 complex under the same conditions[26]). The overall kinetic inertness of the complexes decreases in the order $Cu^{II} >> Zn^{II} > Cd^{II}$. This trend is related to the size of metal ions (fitting to the macrocyclic cavity) and to their affinity for nitrogen or oxygen atoms (strength of the appropriate metal–atom bonds). Although the kinetic lability of the Cu^{II}–H_4L^3 complex prevents its medicinal in vivo use, the studied ligand shows a high potential of dialkyl-bis(methylphosphonic acid) cyclams as promising building blocks of materials/resins for a selective complexation of copper(II). Isolation of copper radioisotopes from a mixture with the other metal isotopes can be realized due to a high selectivity for Cu^{II} complexation at a suitable pH range of 3–4 (compare Figure 3, Figure S2 and Figure S3) where the Cu^{II} ion can be separated from the other ions. After that, the Cu^{II} ion can be released from the resin by elution with a strong acid due to the low kinetic inertness of the given complex.

Experimental Section

General: 1,8-$H_4{}^{Me2}$te2p·$6H_2O$ (H_4L^3·$6H_2O$) was synthesized according to a method described elsewhere[23] or a novel procedure (vide infra). The bis(quarternary) salt **1** (Scheme 2) was prepared according to a literature procedure.[62] NMR spectra were recorded with a Varian NMRS300 spectrometer operating at 300 MHz (^{1}H), 100.6 MHz (^{13}C) and 161.9 MHz (^{31}P) (internal references for ^{1}H and ^{13}C: TMS for $CDCl_3$ solutions and *t*BuOH for D_2O solutions; external reference for ^{31}P: 5% H_3PO_4 in D_2O). Chemical shifts δ are given in ppm and coupling constants J are reported in Hz. Abbreviations s (singlet), d (doublet), t (triplet), quint (quintet) and m (multiplet) are used in order to express the signal multiplicities. For potentiometric titrations, metal nitrates (recrystallized from deionized water) were used, and their stock solutions were standardized by titration with Na_2H_2edta according to the recommended procedure.[63] The stock solution of nitric acid (ca. 0.03 mol dm^{-3}) was prepared from recrystallized KNO_3 on cation-exchange resin (Dowex 50). Carbonate-free KOH stock solution (ca. 0.2 mol dm^{-3}) was standardized against potassium hydrogen phthalate and the HNO_3 solution against the ca. 0.2 mol dm^{-3} KOH solution. The analytical grade chemicals employed in the kinetic studies were purchased from Lachema ($CuCl_2$·$2H_2O$, $ZnCl_2$, $CdCl_2$·$6H_2O$, KOH, CH_3COOH, $ClCH_2COOH$) or Fluka (2-morpholineethanesulfonic acid, MES). The indicators, bromocresol green (Lachema), bromocresol blue (Merck) and 4-(2-pyridylazo)resorcinol (PAR, Lachema), were of the highest available purity. The freshly prepared solutions of $CuCl_2$, $ZnCl_2$ and $CdCl_2$ were standardized by chelatometry.[63]

Synthesis of Tetraethyl 4,11-Dimethyl-1,4,8,11-tetraazacyclotetradecane-1,8-bis(methylphosphonate) (2): Sodium metal (0.184 g, 8 mmol, 4 equiv.) was dissolved in diethyl phosphite (DEP, 5.53 g, 40 mmol, 20 equiv.) in a 100-mL round-bottom flask. The mixture was diluted with dry dmf (30 mL), and bis(quarternary) compound **1** (1.016 g, 2.0 mmol, 1 equiv.) was added portion-wise. The originally formed suspension dissolved over ca. 10 min, and the ^{31}P{^{1}H} and ^{31}P NMR of the reaction mixture showed clear conversion to the final product {$Na^+[^-OP(OEt)_2]$ 145.3 ppm, 8%; product **2** 27.2 ppm, 10%; DEP 10.1 ppm, 80%; HP(O)(ONa)OEt 6.1 ppm, 2%}. The reaction mixture was diluted with aqueous ethanol (10 mL) and poured onto a column of the strong cation exchange resin (Dowex 50, 100 mL, H^+-form) pre-washed with ethanol. The excess of phosphite was eluted with ethanol, and the product was collected by using a concd. aq. NH_3/EtOH (1:10) mixture as the eluent. The fractions containing product were combined and the solvents evaporated to dryness to afford the product as a colourless

oil. Yield 1.03 g (98%). ^{1}H NMR ($CDCl_3$): δ = 1.26 (t, $^3J_{H,H}$ = 7.0 Hz, 12 H, CH_2CH_3), 1.55 (quint, $^3J_{H,H}$ = 6.6 Hz, 4 H, $CH_2CH_2CH_2$), 2.13 (s, 6 H, NCH_3), 2.36 (m, 8 H, CH_2CH_2N), 2.68 (m, 8 H, CH_2CH_2N), 2.82 (d, $^2J_{P,H}$ = 9.9 Hz, 4 H, CH_2P), 4.08 (m, 8 H, OCH_2) ppm. ^{13}C NMR ($CDCl_3$): δ = 16.5 (d, $^3J_{P,C}$ = 6.1 Hz, 4 C, CH_2CH_3), 24.3 (s, 2 C, $CH_2CH_2CH_2$), 43.1 (s, 2 C, NCH_3), 50.5 (d, $^1J_{P,C}$ = 158 Hz, 2 C, PCH_2), 52.2 (d, $^3J_{P,C}$ = 9.4 Hz, 2 C, PCH_2NCH_2), 52.5 (d, $^3J_{P,C}$ = 5.5 Hz, 2 C, PCH_2NCH_2), 54.0 (s, 2 C, CH_2CH_2), 54.7 (s, 2 C, CH_2CH_2), 61.7 (d, $^2J_{P,C}$ = 7.2 Hz, 4 C, OCH_2). ^{31}P NMR ($CDCl_3$): δ = 25.8 (pseudo-sept, $^2J_{P,H} \approx {}^3J_{P,H} \approx 8.5$ Hz) ppm.

Synthesis of 4,11-Dimethyl-1,4,8,11-tetraazacyclotetradecane-1,8-bis(methylphosphonic acid) (1,8-H_4^{Me2}te2p, H_4L^3): The product obtained above was dissolved in 6 M aq. HCl, and the mixture was heated to reflux for 24 h. Isolation according to the reported procedure[23] afforded the title compound as H_4L^3·$6H_2O$ in 96% yield. Characterization data were identical with those reported previously.[23]

X-ray Studies: Selected crystals were mounted on glass fibres in random orientation and cooled to 150(1) K. The diffraction data were collected by employing a Nonius Kappa CCD diffractometer (Enraf–Nonius) using Mo-K_α (λ = 0.71073 Å) at 150(1) K (Cryostream Cooler Oxford Cryosystem) and analyzed by using the HKL DENZO program package.[64] The structures were solved by direct methods and refined by full-matrix least-squares techniques (SIR92[65] and SHELXL97[66]). The used scattering factors for neutral atoms were included in the SHELXL97 program. The crystallographically relevant data are compiled in Table 11. The sample of H_4L^3 was dissolved in 6 M HCl, and the solution was concentrated to dryness. The residue was dissolved in water, and single crystals of (H_6L^3)Cl_2·$4H_2O$ were formed upon a slow concentration of the resulting solution. In the structure of (H_6L^3)Cl_2·$4H_2O$, a structurally independent unit is formed by one half of the ligand molecule, one chloride anion and two solvate water molecules. All non-hydrogen atoms were refined anisotropically. All hydrogen atoms were localized in the electron-density difference map. However, the hydrogen atoms attached to carbon atoms were fixed in theoretical positions, and hydrogen atoms attached to nitrogen and oxygen atoms were fixed in the original positions by using U_{eq}(H) = 1.2U_{eq}(X). Single crystals of the Cu^{II}–H_4L^3 complex were prepared in the following way: H_4L^3·$6H_2O$ (50 mg, 0.095 mmol) and $Cu(NO_3)_2$·$3H_2O$ (36 mg, 0.149 mmol) were dissolved in distilled water (5 mL), and NH_4PF_6 (16 mg, 0.098 mmol) was added. Blue crystals were deposited from this solution upon standing for several days. From the bulk solid, a single crystal was selected and subjected to the X-ray structure determination, showing a composition of [Cu(H_3L^3)][Cu(H_2L^3)]PF_6·$3H_2O$. The elemental analysis of the bulk matter corresponds well with the expected composition with partial loss of the solvate water molecules {[Cu(H_3L^3)][Cu(H_2L^3)]-PF_6·H_2O; M_w = 1119.83; calcd. (found) C 30.03 (30.03), H 6.03 (6.06), N 10.01 (9.61)}. In the structure of [Cu(H_3L^3)][Cu(H_2L^3)]-PF_6·$3H_2O$, an asymmetric unit consists of two complex molecules in different protonation states, one hexafluorophosphate anion and three solvate water molecules. The first complex molecule is triprotonated, i.e. having an overall charge of 1+, and the second one is diprotonated, i.e. non-charged. The positive charge of the first molecule is compensated by the hexafluorophosphate anion. All non-hydrogen atoms were refined anisotropically except for the oxygen atom of one solvate water molecule, which was refined isotropically disordered in two positions with relative occupancy 62:38%. All hydrogen atoms were localized in the electron-density difference map; the hydrogen atoms belonging to the carbon atoms were fixed in theoretical positions and those attached to the oxygen atoms were fixed in the original positions using U_{eq}(H) = 1.2U_{eq}(X). CCDC-728457 [(H_6L^3)Cl_2·$4H_2O$] and -728458 {[Cu(H_3L^3)][Cu(H_2L^3)]PF_6·$3H_2O$} contain the supplementary crystallographic data for this paper. These data can be obtained free of charge from The Cambridge Crystallographic Data Centre via www.ccdc.cam.ac.uk/data_request/cif.

Potentiometry: In general, the experiments followed a well-established procedure.[28] The equilibrium in metal(II)–H_4L^3 systems with all metal ions except for Cu^{II} and Ni^{II} was established quickly in each titration point (less than 2 min) and, thus, they were studied by conventional titrations. A precipitate [probably $Mg(OH)_2$] was formed with Mg^{II} in the alkaline region, and no difference from the free ligand titration curve was seen before the precipitation. The titrations were carried out in a thermostatted vessel at 25.0 ± 0.1 °C, at a constant ionic strength $I(KNO_3)$ = 0.1 mol dm^{-3}, by using a PHM 240 pH-meter, a 2-mL ABU 900 automatic piston burette and a GK 2401B combined glass electrode (all Radiometer). The ligand concentration in the titration vessel was ca. 0.004 mol dm^{-3}. The metal/ligand ratio was 1:1 in all cases except

Table 11. Crystallographic parameters of the studied compounds.

Parameter	(H_6L^3)Cl_2·$4H_2O$	[Cu(H_3L^3)][Cu(H_2L^3)]PF_6·$3H_2O$
Empirical formula	$C_{14}H_{44}Cl_2N_4O_{10}P_2$	$C_{28}H_{71}Cu_2F_6N_8O_{15}P_5$
M_r	561.37	1155.86
Colour, habit	colourless, prism	blue, rod
Crystal system	triclinic	monoclinic
Space group	$P\bar{1}$	$P2_1$
a [Å]	7.5927(3)	9.8304(2)
b [Å]	9.5545(4)	14.8183(3)
c [Å]	10.1917(4)	15.3437(4)
α [°]	104.810(2)	90
β [°]	107.686(2)	93.1543(14)
γ [°]	99.781(3)	90
V [Å^3]	655.95(5)	2231.73(9)
Z	1	2
$D_{calcd.}$ [g cm^{-3}]	1.421	1.720
μ [mm^{-1}]	0.422	1.230
Unique refl.	2300	10194
Obsd. refl. [$I > 2\sigma(I)$]	2117	9467
R; R' [$I > 2\sigma(I)$]	0.0287; 0.0321	0.0321; 0.0377
wR; wR' [$I > 2\sigma(I)$]	0.0699; 0.0721	0.0702; 0.0730

for Ca^{II} where a 5:1 ratio was used to obtain a reasonable abundance of the complex species; in some systems with transition-metal ions, a 2:1 ratio was also titrated but no M_2L species could be successfully included in the chemical model during fitting of data. The initial volume was ca. 5 mL. The measurements were taken with HNO_3 excess added to the initial mixture. The mixtures were titrated with the stock KOH solution in the region of $-\log[H^+]$ = 1.6–12.0. Titrations for each system were carried out at least four times. Each titration consisted of ca. 40 points. The inert atmosphere was provided by a constant passage of argon saturated with water vapour. Copper(II) solutions were titrated under the above conditions except that the waiting time (to obtain a stable potential) was about 15 min for the first point and about 3 min for the next 15 points. The complexation reaction was too slow to be monitored by standard titrations for systems with Ni^{II}. The system was studied by the "out-of-cell" method. The data were collected for 2×25 solutions (two parallel titrations); each solution was mixed separately in the test tube (each sample volume ca. 1 mL) and an appropriate amount of the KOH solution was added to each test tube to simulate the common titration; the region of $-\log[H^+]$ was 1.8–9.0. The tubes were tightly closed and left to equilibrate at room temperature for three weeks (in a separate preliminary experiment, it was found that the titration curves taken after three and six weeks of equilibration were identical). Then, the potential at each titration point (i.e. in each tube) was determined with a freshly calibrated electrode. The constants with their standard deviations were calculated by using the OPIUM program package.[67] The program minimizes the criterion of the generalized least-squares method using the calibration function given in Equation (5).

$$E = E_0 + S \times \log[H^+] + j_1 \times [H^+] + j_2 \times K_W/[H^+] \quad (5)$$

The term E_0 contains the standard potentials of the electrodes used and the contributions of inert ions to the liquid-junction potential. The term S corresponds to the Nernstian slope, and the terms $j_1 \times [H^+]$ and $j_2 \times K_W/[H^+] = j_2 \times [OH^-]$ are contributions of the H^+ and OH^- ions to the liquid-junction potential. It is clear that j_1 and j_2 cause a deviation from a linear dependence of E on $-\log[H^+]$ only in strongly acid and strongly alkaline solutions. The calibration parameters were determined from a titration of the standard HNO_3 solution with the standard KOH solution just before and after each titration of the ligand/metal ion system to give calibration/titration pairs used for calculations of stability constants. The protonation constants β_h of $H_4\mathbf{L^3}$ were taken from the literature[23] and are concentration constants defined as $\beta_h = [H_hL]/[H]^h \times [L]$; they can be transferred to the pK_A values [$pK_1 = \log\beta_1$ and in general $pK_A(H_hL) = \log\beta_h - \log\beta_{(h-1)}$]. The concentration stability constants β_{hlm} are defined as $\beta_{hlm} = [H_hL_lM_m]/\{[H]^h \times [L]^l \times [M]^m\}$. The water ion product pK_W (13.78) and the stability constants of metal hydroxido complexes included in the calculations were taken from the literature.[43,68,69]

Kinetic Measurements: In general, the experiments were run according to published procedures.[28] The formation kinetics experiments were arranged under pseudo-first-order conditions with at least a ten-fold excess of the particular metal ion (chloride salts, $c_M = 1 \times 10^{-3}$ M, $c_L = 1 \times 10^{-4}$ M) except for the experiments where dependences of $^{fM}k_{obs}$ on the metal ion concentration was monitored [$c_M = (1–10) \times 10^{-3}$ M, $c_L = 1 \times 10^{-4}$ M]. The acidity was controlled by HCl, or the solutions were slightly buffered (0.005 M) by chloroacetate, acetate or MES acid/salt buffers. The measurements were done at 25 ± 0.2 °C and at an ionic strength I = 0.1 M (H,K)-Cl. A conventional diode-array spectrophotometer HP 8453A (Hewlett Packard, USA) was used for measurements in the range where the reaction was slow (pH 1.5–3.6 for Cu^{II}; 4.0–5.5 for Zn^{II}; 5.3–5.7 for Cd^{II}). When the formation reaction was fast ($10\tau <$ 10 min), a Bio Sequential SX-17 stopped-flow spectrometer (Applied Photophysics, UK) was used (pH = 4.1–6.0 for Cu^{II}; 6.0–6.8 for Zn^{II}; 5.9–7.0 for Cd^{II}). In these pH regions, the $(H_5\mathbf{L^3})^+$, $H_4\mathbf{L^3}$, $(H_3\mathbf{L^3})^-$ and $(H_2\mathbf{L^3})^{2-}$ species are present in solution (for the ligand distribution diagram, see Figure S1), and these species were considered in the fitting procedure (vide infra). In all cases, the $(H_5\mathbf{L^3})^+$ species could not be successfully included into fits; thus, for Cu^{II} and Cd^{II}, the formation reaction was characterized by rate constants $^{fM}k_{H_4L}$, $^{fM}k_{H_3L}$ and $^{fM}k_{H_2L}$ [Scheme 3, Equation (1)]. In the case of Zn^{II} complexation, the reactivity of the $[Zn(OH)]^+$ complex had to be also included for successful fits of data at pH > 5.5, giving an additional rate constant $^{fZn}k_{OH}$ [Scheme S1, Equation (2)]. For the colourless Zn^{II} and Cd^{II} complexes, the indicator technique was used for detection of the reaction course;[47] the 2×10^{-5} M solutions of indicators [bromocresol green (pH < 5.2) or bromocresol blue (pH > 5.2)] were used for visualization. The complexation of Cu^{II} was monitored directly by an increase of the CT band (λ = 310 nm). The dissociation kinetics of $[Cu(\mathbf{L^3})]^{2-}$ were studied in the $[H^+]$ range 0.05–1.25 M, at an ionic strength of I = 5.0 M (H,Na)ClO_4, with a starting Cu^{II}–$H_4\mathbf{L^3}$ complex concentration $c = 1 \times 10^{-4}$ M and in the temperature range 20–35 °C. The reaction was monitored by a decrease of the intensity of the CT band (λ = 310 nm) of the complex with time. Dissociation of the $[Zn(\mathbf{L^3})]^{2-}$ and $[Cd(\mathbf{L^3})]^{2-}$ complexes ($c = 1 \times 10^{-3}$ M) were measured in the pH range 3.5–6.1 at 25 °C (I = 0.1 M KCl). A copper(II) ion (chloride salt, $c_{Cu} = 1 \times 10^{-3}$ M, λ = 310 nm) was used as a ligand scavenger in decomplexation kinetics of both complexes. The kinetic measurements were carried out with a diode-array spectrophotometer HP 8453A (Hewlett Packard, USA) for slow kinetics ($10\tau >$ 10 min) and a Bio Sequential SX-17 stopped-flow spectrometer (Applied Photophysics, UK) for fast kinetics ($10\tau <$ 10 min). The measured values of absorbance were corrected for the background analytical signal. The values of k_{obs} were calculated from the experimental data by a single-exponential model with HP software and Excel[70] software with identical results. Fitting of pH and temperature dependences of rate constants was performed by using the MicroMath Scientist program[71] with typically the $1/y^2$ weighting scheme.

Supporting Information (see footnote on the first page of this article): Distribution diagram of free ligand $H_4\mathbf{L^3}$. Distribution diagrams of Co^{II}– and Ni^{II}–$H_4\mathbf{L^3}$ systems. Examples of dependence of $^{fCu}k_{obs}$ (measured at constant pH) on copper(II) concentration and logarithmic analysis of experimental data. pH dependence of the second-order rate constants for the formation of Cu^{II}–, Zn^{II}– and Cd^{II}–$H_4\mathbf{L^1}$ and –$H_4\mathbf{L^3}$ complexes. The dependence of the observed rate constants $^{dM}k_{obs}$ for the dissociation of Cu^{II}–, Zn^{II}– and Cd^{II}–$H_4\mathbf{L^1}$ and –$H_4\mathbf{L^3}$ complexes on $[H^+]$ or pH. Derivation of the equations used for fitting of formation kinetics data. Comparison of kinetic parameters of acid-assisted dissociation of copper(II) complexes of $H_2\mathbf{L^1}$ and $H_2\mathbf{L^3}$.

Acknowledgments

We thank Dr. K. Lang (Institute of Inorganic Chemistry, Academy of Sciences of the Czech Republic) for the use of a stopped-flow apparatus and Dr. I. Císařová for X-ray data acquisition. This work was supported by the Ministry of Education of the Czech Republic (ME09065 and MSM0021620857) and the Grant Agency of the Czech Republic (203/09/1056). This work was carried out within the framework of the COST D38 and BM607 projects and EU

FP6 Network of Excellence EMIL (LSHC-2004-503569) and DiMI (LSHB-2005-512146) projects.

[1] M. Meyer, V. Dahaoui-Ginderey, C. Lecomte, R. Guilard, *Coord. Chem. Rev.* **1998**, *178–180*, 1313–1405.
[2] L. F. Lindoy, *Adv. Inorg. Chem.* **1998**, *45*, 75–125.
[3] R. Delgado, V. Félix, L. M. P. Lima, D. W. Price, *Dalton Trans.* **2007**, 2734–2745.
[4] A. E. Merbach, É. Tóth (Eds.), *The Chemistry of Contrast Agents in Medical Magnetic Resonance Imaging*, Wiley, Chichester, UK, **2001**.
[5] *Topics in Current Chemistry*, Springer, Heidelberg, Germany, **2002**, vol. 221.
[6] S. Aime, M. Botta, E. Terreno, *Adv. Inorg. Chem.* **2005**, *57*, 173–237.
[7] P. Caravan, *Chem. Soc. Rev.* **2006**, *35*, 512–523.
[8] P. Hermann, J. Kotek, V. Kubíček, I. Lukeš, *Dalton Trans.* **2008**, 3027–3047.
[9] C. J. Anderson, M. J. Welch, *Chem. Rev.* **1999**, *99*, 2219–2234.
[10] W. A. Volkert, T. J. Hoffmann, *Chem. Rev.* **1999**, *99*, 2269–2292.
[11] a) S. Liu, *Chem. Soc. Rev.* **2004**, *33*, 445–461; b) S. Liu, D. S. Edwards, *Bioconjugate Chem.* **2001**, *12*, 7–34.
[12] M. J. Welch, C. S. Redvanly (Eds.), *Handbook of Radiopharmaceuticals – Radiochemistry and Applications*, Wiley, Chichester, UK, **2003**.
[13] W. P. Li, L. A. Meyer, C. J. Anderson, *Top. Curr. Chem.* **2005**, *252*, 179–192.
[14] S. V. Smith, *J. Inorg. Biochem.* **2004**, *98*, 1874–1901.
[15] X. Sun, C. J. Anderson, *Methods Enzymol.* **2004**, *386*, 237–261.
[16] T. J. Wadas, E. H. Wong, G. R. Weisman, C. J. Anderson, *Curr. Pharm. Des.* **2007**, *13*, 3–16.
[17] X. Liang, P. J. Sadler, *Chem. Soc. Rev.* **2004**, *33*, 246–266.
[18] L. A. Bass, M. Wang, M. J. Welch, C. J. Anderson, *Bioconjugate Chem.* **2000**, *11*, 527–532.
[19] a) E. H. Wong, G. R. Weisman, D. C. Hill, D. P. Reed, M. E. Rogers, J. P. Condon, M. A. Fagan, J. C. Calabrese, K.-C. Lam, I. A. Guzei, A. L. Rheingold, *J. Am. Chem. Soc.* **2000**, *122*, 10561–10572; b) X. Sun, M. Wuest, G. R. Weisman, E. H. Wong, D. P. Reed, C. A. Boswell, R. J. Motekaitis, A. E. Martell, M. J. Welch, C. J. Anderson, *J. Med. Chem.* **2002**, *45*, 469–477; c) C. A. Boswell, X. Sun, W. Niu, G. R. Weisman, E. H. Wong, A. L. Rheingold, C. J. Anderson, *J. Med. Chem.* **2004**, *47*, 1465–1474; d) K. S. Woodin, K. J. Heroux, C. A. Boswell, E. H. Wong, G. R. Weisman, W. J. Niu, S. A. Tomellini, C. J. Anderson, L. N. Zakharov, A. L. Rheingold, *Eur. J. Inorg. Chem.* **2005**, 4829–4833; e) C. A. Boswell, P. McQuade, G. R. Weisman, E. H. Wong, C. J. Anderson, *Nucl. Med. Biol.* **2005**, *32*, 29–38.
[20] a) W. Niu, E. H. Wong, G. R. Weisman, L. N. Zakharov, C. D. Incarvito, A. L. Rheingold, *Polyhedron* **2004**, *23*, 1019–1025; b) J. E. Sprague, Y. Peng, A. L. Fiamengo, K. S. Woodin, E. A. Southwick, G. R. Weisman, E. H. Wong, J. A. Golen, A. L. Rheingold, C. J. Anderson, *J. Med. Chem.* **2007**, *50*, 2527–2535.
[21] K. J. Heroux, K. S. Woodin, D. J. Tranchemontagne, P. C. B. Widger, E. Southwick, E. H. Wong, G. R. Weisman, S. A. Tomellini, T. J. Wadas, C. J. Anderson, S. Kassel, J. A. Golen, A. L. Rheingold, *Dalton Trans.* **2007**, 2150–2162.
[22] C. A. Boswell, C. A. S. Regino, K. E. Baidoo, K. J. Wong, A. Bumb, H. Xu, D. E. Milenic, J. A. Kelley, C. C. Lai, M. W. Brechbiel, *Bioconjug. Chem.* **2008**, *19*, 1476–1484.
[23] J. Kotek, P. Vojtíšek, I. Císařová, P. Hermann, P. Jurečka, J. Rohovec, I. Lukeš, *Collect. Czech. Chem. Commun.* **2000**, *65*, 1289–1316.
[24] J. Kotek, P. Vojtíšek, I. Císařová, P. Herman, I. Lukeš, *Collect. Czech. Chem. Commun.* **2001**, *66*, 363–381.
[25] J. Kotek, I. Císařová, P. Hermann, I. Lukeš, J. Rohovec, *Inorg. Chim. Acta* **2001**, *317*, 324–330.
[26] a) J. Kotek, P. Lubal, P. Hermann, I. Císařová, I. Lukeš, T. Godula, I. Svobodová, P. Táborský, J. Havel, *Chem. Eur. J.* **2003**, *9*, 233–248; b) P. Lubal, J. Maleček, P. Hermann, J. Kotek, J. Havel, *Polyhedron* **2006**, *25*, 1884–1892.
[27] B. Bosnich, C. K. Poon, M. Tobe, *Inorg. Chem.* **1965**, *4*, 1102–1108.
[28] I. Svobodová, P. Lubal, J. Plutnar, J. Havlíčková, J. Kotek, P. Hermann, I. Lukeš, *Dalton Trans.* **2006**, 5184–5197.
[29] I. Svobodová, P. Lubal, P. Hermann, J. Kotek, J. Havel, *J. Inclusion Phenom. Macrocycl. Chem.* **2004**, *49*, 11–15.
[30] I. Svobodová, P. Lubal, P. Hermann, J. Kotek, J. Havel, *Microchim. Acta* **2004**, *148*, 21–26.
[31] T. Vitha, J. Kotek, J. Rudovský, V. Kubíček, I. Císařová, P. Hermann, I. Lukeš, *Collect. Czech. Chem. Commun.* **2006**, *71*, 337–367.
[32] J. Havlíčková, H. Medová, T. Vitha, J. Kotek, I. Císařová, P. Hermann, *Dalton Trans.* **2008**, 5378–5386; and unpublished results.
[33] S. Füzerová, J. Kotek, I. Císařová, P. Hermann, K. Binnemans, I. Lukeš, *Dalton Trans.* **2005**, 2908–2915.
[34] a) I. M. Helps, D. Parker, J. Chapman, G. Ferguson, *J. Chem. Soc., Chem. Commun.* **1988**, 1094–1095; b) J. Chapman, G. Ferguson, J. F. Gallagher, M. C. Jennings, D. Parker, *J. Chem. Soc., Dalton Trans.* **1992**, 345–353.
[35] a) A. Comparone, T. A. Kaden, *Helv. Chim. Acta* **1998**, *81*, 1765–1772; b) L. Siegfried, A. Comparone, M. Neuburger, T. A. Kaden, *Dalton Trans.* **2005**, 30–36.
[36] a) H. Kurosaki, C. Bucher, E. Espinosa, J.-M. Barbe, R. Guilard, *Inorg. Chim. Acta* **2001**, *322*, 145–149; b) C. Bucher, E. Duval, J.-M. Barbe, J.-N. Verpeaux, C. Amatore, R. Guilard, *C. R. Acad. Sci., Ser. IIc Chem.* **2000**, *3*, 211–222.
[37] a) A. E. Goeta, J. A. K. Howard, D. Maffeo, H. Puschmann, J. A. G. Williams, D. S. Yufit, *J. Chem. Soc., Dalton Trans.* **2000**, 1873–1880; b) A. S. Batsanov, A. E. Goeta, J. A. K. Howard, D. Maffeo, H. Puschmann, J. A. G. Williams, *Polyhedron* **2001**, *20*, 981–986.
[38] C. Bucher, E. Duval, E. Espinoza, J. M. Barbe, J. N. Verpeaux, C. Amatore, R. Guilard, *Eur. J. Inorg. Chem.* **2001**, 1077–1079.
[39] L. M. P. Lima, R. Delgado, M. G. B. Drew, P. Brandão, V. Félix, *Dalton Trans.* **2008**, 6593–6608.
[40] A. W. Addison, T. N. Rao, J. Reedijk, J. van Rijn, G. C. Verschoor, *J. Chem. Soc., Dalton Trans.* **1984**, 1349–1356.
[41] I. Lukeš, J. Kotek, P. Vojtíšek, P. Hermann, *Coord. Chem. Rev.* **2001**, *216–217*, 287–312.
[42] R. D. Hancock, R. J. Motekaitis, J. Mashishi, I. Cukrowski, J. H. Reibenspies, A. E. Martell, *J. Chem. Soc. Perkin Trans. 2* **1996**, 1925–1929.
[43] a) A. E. Martell, R. M. Smith, *Critical Stability Constants*, Plenum Press, New York, **1974–1989**, vols. 1–6; b) *NIST Standard Reference Database 46* (Critically Selected Stability Constants of Metal Complexes), Version 7.0, **2003**.
[44] a) S. Chaves, R. Delgado, J. J. R. Frausto Da Silva, *Talanta* **1992**, *39*, 249–254; b) R. Delgado, J. Costa, K. P. Guerra, L. M. P. Lima, *Pure Appl. Chem.* **2005**, *77*, 569–579.
[45] a) R. Delgado, L. C. Siegfried, T. A. Kaden, *Helv. Chim. Acta* **1990**, *73*, 140–148; b) F. Marques, L. Gano, M. P. Campello, S. Lacerda, I. Santos, L. M. P. Lima, J. Costa, P. Antunes, R. Delgado, *J. Inorg. Biochem.* **2006**, *100*, 270–280.
[46] S. A. Pisareva, F. I. Belskii, T. Ya. Medved, M. I. Kabachnik, *Izv. Akad. Nauk SSSR, Ser. Khim.* **1987**, 413–417.
[47] S. P. Kasprzyk, R. G. Wilkins, *Inorg. Chem.* **1982**, *21*, 3349–3352.
[48] R. G. Wilkins, *Kinetics and Mechanism of Reactions of Transition Metal Complexes*, VCH, Weinheim, **1991**.
[49] a) F. Cuenot, M. Meyer, E. Espinosa, R. Guilard, *Inorg. Chem.* **2005**, *44*, 7895–7910; b) F. Cuenot, M. Meyer, E. Espinosa, A. Bucaille, R. Burgat, R. Guilard, C. Marichal-Westrich, *Eur. J. Inorg. Chem.* **2008**, 267–283.
[50] R. Buxtorf, T. A. Kaden, *Helv. Chim. Acta* **1974**, *57*, 1035–1042.

[51] N. McCann, G. A. Lawrance, Y.-M. Neuhold, M. Maeder, *Inorg. Chem.* **2007**, *46*, 4002–4009.
[52] M. Kodama, E. Kimura, *J. Chem. Soc., Dalton Trans.* **1977**, 1473–1478.
[53] M. Maeder, Y.-M. Neuhold, G. Puxty, P. King, *Phys. Chem. Chem. Phys.* **2003**, *5*, 2836–2841.
[54] A. P. Leugger, L. Hertli, T. A. Kaden, *Helv. Chim. Acta* **1978**, *61*, 2296–2306.
[55] K.-Y. Choi, *Polyhedron* **1997**, *16*, 2073–2079.
[56] M. Kodama, E. Kimura, *J. Chem. Soc., Dalton Trans.* **1976**, 116–120.
[57] M. Kodama, E. Kimura, *J. Chem. Soc., Dalton Trans.* **1977**, 2269–2276.
[58] L. Hertli, T. A. Kaden, *Helv. Chim. Acta* **1974**, *57*, 1328–1333.
[59] F. A. Dunand, L. Helm, A. E. Merbach, *Adv. Inorg. Chem.* **2003**, *54*, 1–69.
[60] H. Elias, *Coord. Chem. Rev.* **1999**, *187*, 37–73.
[61] L.-H. Chen, C.-S. Chung, *Inorg. Chem.* **1988**, *27*, 1880–1883.
[62] G. Royal, V. Dahaoui-Gindrey, S. Dahaoui, A. Tabard, R. Guilard, P. Pulumbi, C. Lecomte, *Eur. J. Org. Chem.* **1998**, 1971–1975.
[63] a) R. Přibil, *Analytical Applications of EDTA and Related Compounds*, Pergamon Press, Oxford, UK, **1972**; b) G. Schwarzenbach, H. Flaschka, *Complexometric Titrations*, Methuen, London, UK, **1969**.
[64] a) Z. Otwinovski, W. Minor, *HKL Denzo and Scalepack Program Package*, Nonius BV, Delft, **1997**; b) Z. Otwinovski, W. Minor, *Methods Enzymol.* **1997**, *276*, 307–326.
[65] A. Altomare, M. C. Burla, M. Camalli, G. Cascarano, C. Giacovazzo, A. Guagliardi, G. Polidori, *J. Appl. Crystallogr.* **1994**, *27*, 435.
[66] G. M. Sheldrick, *SHELXL97, Program for Crystal Structure Refinement from Diffraction Data*, University of Gottingen, Gottingen, Germany, **1997**.
[67] a) M. Kývala, I. Lukeš, *Chemometrics '95*, Abstract book, Pardubice, Czech Republic, **1995**, p. 63; b) M. Kývala, P. Lubal, I. Lukeš, *IX. Spanish-Italian and Mediterranean Congress on Thermodynamics of Metal Complexes (SIMEC 98)*, Girona, Spain, **1998**. Full version of *OPIUM program package* is available (free of charge) from http://www.natur.cuni.cz/~kyvala/opium.html.
[68] C. F. Baes Jr, R. E. Mesmer, *The Hydrolysis of Cations*, Wiley, New York, NY, **1976**.
[69] Y. Zhang, M. Muhammed, *Hydrometallurgy* **2001**, *60*, 215–236.
[70] E. J. Billo, *Excel for Chemists*, Wiley-VCH, New York, NY, **2001**.
[71] *Scientist for Windows version 2.01*, Micromath Inc., Salt Lake City, UT, **1995**.

Received: April 20, 2009
Published Online: July 21, 2009

